Angewandte Chemie
Eine Zeitschrift der Gesellschaft Deutscher Chemiker

Supporting Information

# Effect of Hydrophilic Monomer Distribution on Self-Assembly of a pH-Responsive Copolymer: Spheres, Worms and Vesicles from a Single Copolymer Composition

*Junliang Zhang, Barbara Farias-Mancilla, Ihor Kulai, Stephanie Hoeppener, Barbara Lonetti, Sylvain Prévost, Jens Ulbrich, Mathias Destarac, Olivier Colombani, Ulrich S. Schubert,* Carlos Guerrero-Sanchez,* and Simon Harrisson**

anie_202010501_sm_miscellaneous_information.pdf

# CONTENTS

## 1. MATERIALS AND METHODS.

***Materials.*** 1,4-Dioxane, dichloromethane (DCM), acetone, and methanol were purchased from TCI and used as received. 1,1′-Azobis(cyclohexanecarbonitrile) (ACHN), trifluoroacetic acid (TFA), azobisisobutyronitrile (AIBN), and anisole were purchased from Sigma Aldrich and used as received. Butyl acrylate (BA) and *tert*-butyl acrylate (*t*BA) were bought from TCI and stirred with inhibitor remover (purchased from Sigma Aldrich) for 30 minutes before use. Cyanomethyl dodecyl trithiocarbonate (CTA) was purchased from Strem Chemicals, lnc. and used as received. Methanol and distilled water were used for polymer precipitation. 1,3,5-trioxane was purchased from Sigma Aldrich and used as received. $CDCl_3$, DMSO-$d_6$, and acetone-$d_6$ obtained from Eurisotop were used as solvent for $^1$H NMR analysis.

***Proton Nuclear Magnetic Resonance ($^1$H NMR) Spectroscopy.*** Spectra were recorded on a Bruker Avance 300 MHz spectrometer at 27 °C in $CDCl_3$ or Acetone-$d_6$. Chemical shift values ($\delta$) are reported in ppm. The residual proton signal of the solvent ($\delta_H$ = 7.26 ppm in $CDCl_3$, $\delta_H$ = 2.05 ppm in Acetone-$d_6$) was used as internal reference. Monomer conversions were determined by comparing the integration of the vinyl protons ($\delta$ ~ 6.50–5.50 ppm) before and after reaction, using 1,3,5-trioxane as an internal standard. The theoretical number average molar mass ($M_{\mathrm{n,th}}$) is calculated from equation S1:

$$M_{\mathrm{n,th}} = \frac{[\mathrm{M}]_0\, p M_M}{[\mathrm{CTA}]_0} + M_{\mathrm{CTA}} \qquad \text{(S1)}$$

where $[\mathrm{M}]_0$ and $[\mathrm{CTA}]_0$ are the initial concentrations (in mol $L^{-1}$) of monomer and chain transfer agent respectively; $p$ is the monomer conversion as determined by $^1$H NMR, $M_{\mathrm{M}}$ and $M_{\mathrm{CTA}}$ are the molar masses (g $mol^{-1}$) of the monomer and chain transfer agent respectively.

***Size Exclusion Chromatography (SEC).*** Number-average molar masses ($M_{\mathrm{n,SEC}}$) and dispersities ($Đ$) of polymers were determined using SEC.

**SEC system in Laboratoire des IMRCP, University of Toulouse**: The SEC analyses were conducted on a system composed of Waters 515 HPLC pump, Agilent 1260 Autosampler, Varian ProStar 500 column valve module, set of three Waters columns (Styragel Guard Column, 20 µm, 4.6 mm × 30 mm, Styragel HR3, 5 µm, 7.8 mm × 300 mm and Styragel HR4E, 5 µm, 7.8 mm × 300 mm), Varian ProStar 325 UV-Vis detector set at 290 nm and Wyatt Optilab rEX differential refractive index detector using tetrahydrofuran (THF) as an eluent at a flow rate of 1.0 mL min$^{-1}$ (35 °C). The column system was calibrated with PMMA standards (ranging from 1120 to 138600 g mol$^{-1}$). Samples were diluted to a concentration about 2.5 mg mL$^{-1}$ and filtered through 0.45 µm Nylon syringe filters before injection.

**SEC system in IOMC, JCSM, Friedrich Schiller University Jena**: The measurements were performed on a Shimadzu system equipped with a CBM-20A system controller, an LC-10AD VP pump, a RID-10A refractive index detector and a PSS SDV column. The eluent was chloroform/isopropanol/trimethylamine (94%/2%/4%, v/v/v). Samples were run at 1 mL min$^{-1}$ at 40 °C. Poly(methyl methacrylate) standards (molar mass range is ca. 400 – 100000 g mol$^{-1}$) were used for calibration. Analyzed samples were filtered through a PVDF membrane with 0.22 µm pore size before injection.

### ***Potentiometric Titration***

Preparation of the solutions. For the titration of block, asymmetric diblock, asymmetric triblock and gradient copolymers of 20 000 g.mol$^{-1}$ (B20, D20, T20, and G20), 30 mL of polymer solution at $C_{polymer}$ = 1 g.L$^{-1}$ (corresponding to [AA] = 5 x10$^{-3}$ mol.L$^{-1}$) and [NaCl] = 0.1 M were prepared as follows. The degree of ionization, $\alpha$, of the polymers in their solid form was 0. The polymers were first dissolved in water in the presence of ~1.1 equivalent of NaOH relative to the total amount of AA units, which was calculated from the chemical structure of the polymer. After stirring for at least one night, the polymers were fully dispersed resulting in transparent solutions. The NaCl concentration was then adjusted using a 4 M NaCl solution.

Potentiometric titration. The polymer solutions were back titrated at room temperature with [HCl] = 0.1 M using an automatic titrator (TIM 856, Radiometer Analytical) controlled by the TitraMaster 85 software following a procedure published elsewhere.[S1] The addition of HCl titrant was done at a constant speed of 0.1 mL/min. Raw titration data yielded the evolution of the pH of the solution as a function of the volume of titrant. From these data, the total amount of titrable AA units was determined and the evolution of the pH of the solution was plotted as a function of $\alpha$. Details of the data treatment are given elsewhere.[S1]

***Dynamic Light Scattering (DLS).*** Hydrodynamic diameters ($D_h$) and size distributions were determined by DLS on a MALVERN Zetasizer Nano ZS operating at 20 °C with a 633 nm laser module. Measurements were made at a detection angle of 173° (back scattering). Measurements were repeated three times with automatic attenuation selection and measurement position. The average result of these three measurements was used for the manuscript. The results were analyzed using Malvern DTS 6.20 software, using the multiple narrow modes setting. Size distributions were obtained using the CONTIN algorithm. The Z-average diameter ($D_h$) and the width of the distribution as the polydispersity index of the particles (PDI) were obtained by the cumulants method assuming a spherical shape of the particles.

***Cryogenic Transmission Electron Microscopy (Cryo-TEM).*** The polymer solutions (2 mg $mL^{-1}$) obtained by direct dispersion into buffers were used for Cryo-TEM imaging directly. The measurements were performed on an FEI Tecnai $G^2$ 20 platform with a LaB6 filament at 200 kV acceleration voltage. Samples were prepared on Quantifoil grids (R2/2) which were treated with Ar plasma prior to use for hydrophilization and cleaning. 8.5 μL of the solutions (2 mg $mL^{-1}$) was applied onto the grids utilizing an FEI Vitrobot Mark IV system (offset: −5 mm, blotting time: 1 s). After blotting, the samples were immediately plunged into liquid ethane to obtain vitrification. Samples were transferred to a Gatan cryo stage and subsequently into a Gatan cryo holder (Gatan 626) and were transferred into the microscope by always maintaining a temperature below −168 °C during the whole transfer and measurement process after vitrification. Images were acquired with a Mega View (OSIS, Olympus Soft Imaging Systems) or an Eagle 4k CCD camera.

Due to the amount of effort required for the Cryo-TEM measurements and the large number of samples, only selected samples were imaged by Cryo-TEM. Based on the DLS results, B20, G20, D10, and T10 were selected for the Cryo-TEM.

***Small-Angle Neutron Scattering.*** Small-angle neutron scattering (SANS) was performed at the D11 beamline of the Institut Laue-Langevin (ILL) in Grenoble, France.[S2] The SANS patterns were collected using a 2D detector then integrated to obtain the scattering intensity as a function of scattering vector $q = 4\pi \sin(\theta/2)/\lambda$, where $\theta$ is the angle between the incident beam and the detector and $\lambda$ is the neutron wavelength. The measured SANS profiles were normalized to an absolute scale using $H_2O$ as a secondary standard. A combination of four configurations with three different sample-to-detector distances 1.4 m, 8 m and 39 m and two wavelengths (λ=5 Å and 20 Å, FWHM 9%) was employed, covering a total $q$-range from 5 $10^{-3}$ and 5 $nm^{-1}$. The solutions (all in $D_2O$) were loaded in 2 mm quartz cells. The background sample ($D_2O$) was subtracted from the experimental data. Sample concentration was 2 mg $mL^{-1}$.

The software package BerSANS[S3] is used to integrate and merge the data acquired at all configurations and subtract the background. In this way the absolute scattering intensity $d\sigma(q)/d\Omega$ is obtained (eq. S2):

$$\frac{d\sigma(q)}{d\Omega} = n\Delta\rho^2 V^2 P(q) \tag{S2}$$

$n$ is the particle number density, $\Delta\rho$ the difference between the scattering length density of the self-assemblies and the solvent, V the volume of the nano-objetcs. *P(q)* is the particle Form factor.

## 2. SELECTION OF COMPOSITION PROFILES FOR D AND T

The copolymers D and T were intended to be simple structures containing only two or three blocks that nevertheless closely mimicked the gradient composition profile. In order to do so, copolymers were designed which matched both the overall composition of the gradient copolymer (50% acrylic acid) and also the average location of acrylic acid units within the polymer chain.

The gradient copolymer G has a linear composition profile ranging from 100% acrylic acid to 0% acrylic acid. Its overall composition is 50% acrylic acid. The average position of the acrylic acid units, measured from the acrylic acid-rich terminus is given by equation S3:

$$\overline{x_G} = \frac{\int_0^1 x(1-x)\,dx}{\int_0^1 (1-x)\,dx} = \frac{1}{3} \approx 0.33 \tag{S3}$$

D consists of two blocks of equal length, containing 84% and 16% acrylic acid respectively. Its overall composition in acrylic acid is 50%. The average position of the acrylic acid units, measured from the acrylic acid-rich terminus is given by equation S4:

$$\overline{x_D} = \frac{\int_0^{0.5} 0.84x\,dx + \int_{0.5}^{1} 0.16x\,dx}{\int_0^{0.5} 0.84\,dx + \int_{0.5}^{1} 0.16\,dx} = 0.33 \tag{S4}$$

T consists of two short terminal blocks of PAA and PBA respectively, each corresponding to 21% of the total length of the polymer. The central block, corresponding to the remaining 58% of the polymer, is a 50% statistical copolymer of AA and BA. The overall composition in acrylic acid is 50%. The average position of the acrylic acid units, measured from the acrylic acid-rich terminus is given by equation S5:

$$\overline{x_T} = \frac{\int_0^{0.21} x\,dx + \int_{0.21}^{0.79} 0.5x\,dx}{\int_0^{0.21} 1\,dx + \int_{0.21}^{0.79} 0.5x\,dx} = 0.33 \tag{S5}$$

Thus D, T and G share both their overall composition and the average location of acrylic acid units in the chain. For comparison, the average location of the acrylic acid units in the block copolymer B consisting of equal parts polyacrylic acid and polybutyl acrylate is given by equation S6:

$$\overline{x_B} = \frac{\int_0^{0.5} x\,dx}{\int_0^{0.5} 1\,dx} = 0.25 \tag{S6}$$

While that of the statistical copolymer containing 50% acrylic acid units ($S_{50\%}$) is given by equation S7:

`

$$\overline{x_S} = \frac{\int_0^1 0.5x\ dx}{\int_0^1 0.5\ dx} = 0.5 \tag{S7}$$

## 3. REACTIVITY DETERMINATION OF BA AND *t*BA

The copolymerizations were performed in a Chemspeed Accelerator SLT automated parallel synthesizer using a sequential reagent addition and similar experimental protocols as reported elsewhere.[S4-S7]

A stock solution of CTA (100 mg mL$^{-1}$ in dioxane) and AIBN (0.86 mg mL$^{-1}$ in dioxane) was prepared. This solution, *t*BA, and BA were transferred into different containers and placed inside the automated synthesizer. Aliquots of the prepared stock solution of CTA and AIBN, *t*BA, BA, and solvent were transferred from the containers into different reactors (100 mL) of the synthesizer with the automated liquid handling system to provide *t*BA/BA ratios of 16/84, 50/50 and 84/16, overall monomer concentration of 4 mol L$^{-1}$, a monomer:CTA:AIBN ratio of 60:1:0.02 and a final volume of 10 mL (please note that volume changes due to mixing of the reagents have been neglected). 1,3,5-Trioxane was added as internal standard at a concentration of 10 mg mL$^{-1}$ of total reaction volume. Each reactor was degassed in the parallel synthesizer by sparging with inert gas ($N_2$) for 15 min at 0 °C in parallel. Thereafter, the reaction mixtures were heated to 60 °C. Aliquots were taken periodically for $^1$H NMR (0.075 mL) analysis under an inert gas flow. The conversion of each monomer as a function of time was determined by $^1$H NMR analysis and the results are shown in Figure S1.

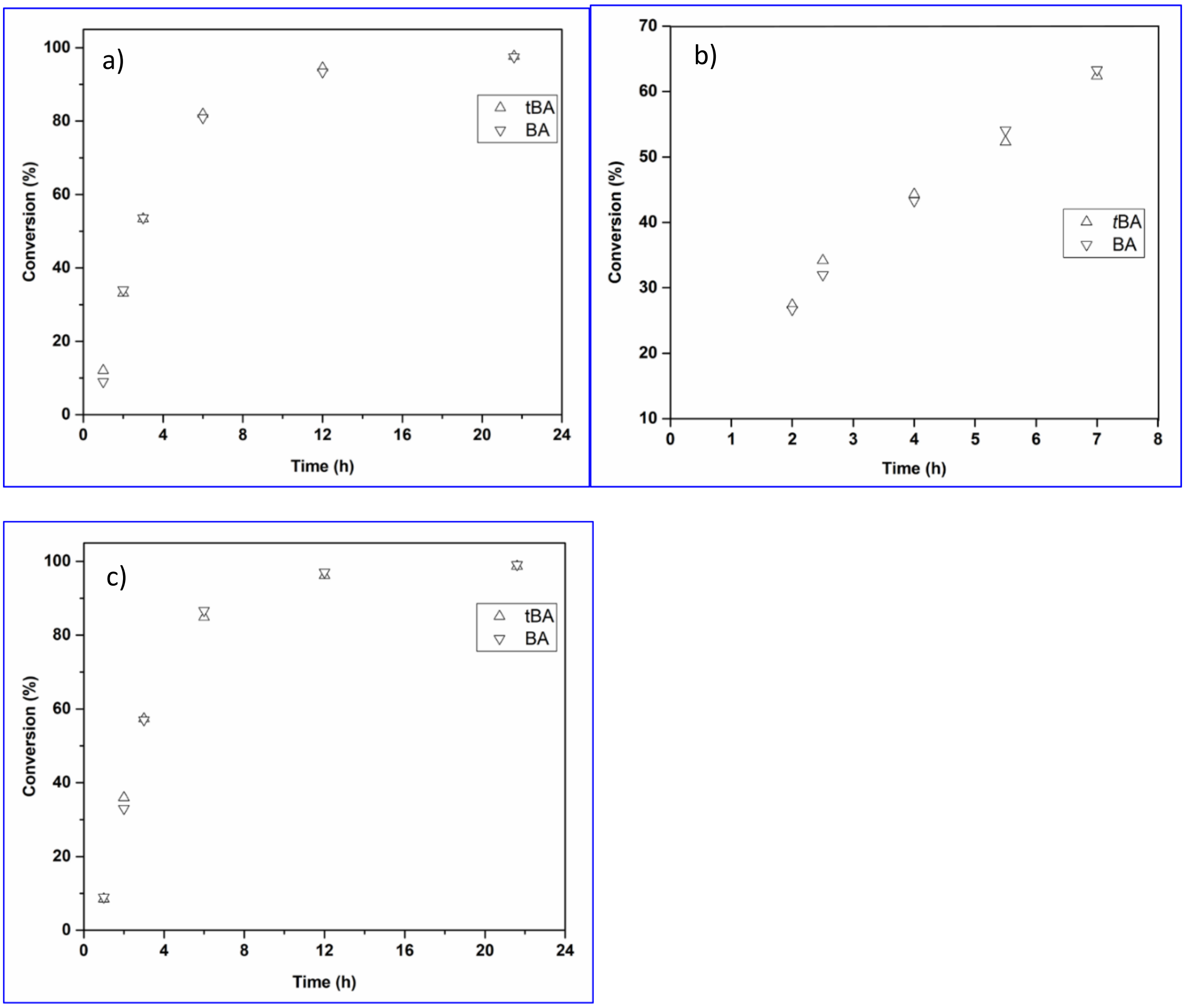

**Figure S1.** Kinetics of copolymerization of tBA and BA at 60°C determined by $^1$H NMR: *t*BA/BA = (a) 16/84, (b) 50/50, (c) 84/16 mol/mol.

## 4. COPOLYMER SYNTHESIS

***Synthesis of block copolymers (poly(BA-block-tBA) (B10 and B20).***

***Stock solution A:*** CTA (1.27 g, 4.00 mmol) and AIBN (0.066 g, 0.40 mmol) were dissolved in 1,4-dioxane (29.5 g, 28.6 mL, 335 mmol) giving a solution with total volume of 30 mL. This stock solution was frozen at 3 °C and melted before use.

***Stock solution B:*** AIBN (0.066 g, 0.40 mmol) was dissolved in 1,4-dioxane (30.8 g, 29.9 mL, 350 mmol) giving a solution with total volume of 30 mL. This stock solution was frozen at 3 °C and melted before use.

BA (1.34 g, 1.5 mL, 10.45 mmol) was mixed with stock solution A (1.00 and 2.00 mL for $M_n$ = 20000 and 10000 g mol$^{-1}$, respectively) in 15 mL vial, adjusted with 1,4-dioxane (2.5 and 1.5 mL for $M_n$ = 20000 and 10000 g mol$^{-1}$, respectively) to 5 mL volume and sealed with a rubber septum. The resulting solution was degassed by purging with Ar for 15 minutes and immersed into a thermostated heating block at 60°C for 8h. An aliquot was evaporated under vacuum and analyzed with SEC. The reaction mixture was concentrated under vacuum to remove any unreacted monomer, precipitated in 10% water in methanol and dried under deep vacuum. Then *t*BA (1.34 g, 1.5 mL, 10.45 mmol) and stock solution B (1.00 and 2.00 mL for $M_n$ = 20000 and 10000 g mol$^{-1}$, respectively) were added, adjusted with 1,4-dioxane (2.00 and 1.00 mL for $M_n$ = 20000 and 10000 g mol$^{-1}$, respectively) to 5 mL volume, degassed by purging with Ar and polymerized by heating at 60°C for 8h following the method described above. The reaction mixture was concentrated under vacuum to remove any unreacted monomer, precipitated in 10% water in methanol and dried under deep vacuum. SEC traces for both block copolymers are shown in Figure S2.

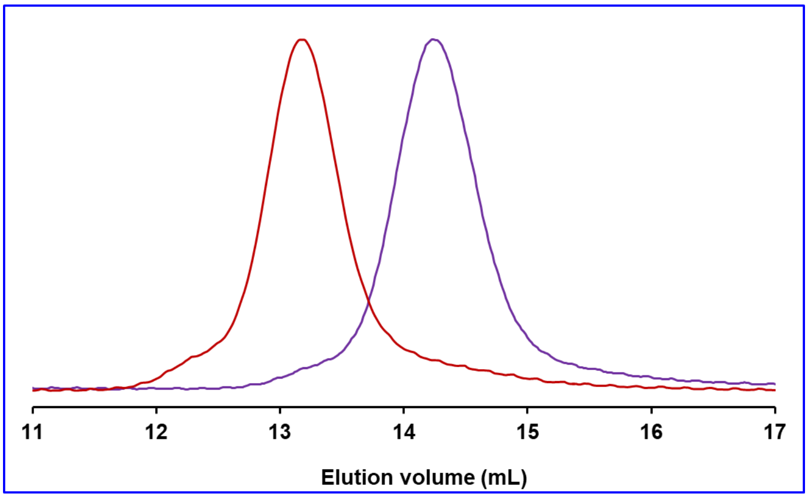

**Figure S2.** Molar mass distributions (SEC RI traces in $CHCl_3$) for the block copolymers polyBA-*block*-poly*t*BA B10 (right) and B20 (left). Samples were analyzed in SEC system in Laboratoire des IMRCP, University of Toulouse.

### *Synthesis of asymmetric diblock copolymers (poly(tBA$_{84\%}$-ran-BA$_{16\%}$)-b-poly(tBA$_{16\%}$-ran-BA$_{84\%}$) (D10 and D20).*

Copolymerizations were performed in a Chemspeed Accelerator SLT automated parallel synthesizer using a sequential reagent addition and similar experimental protocols as reported elsewhere.[S4-S7]

**First block:** A stock solution of CTA (100 mg mL$^{-1}$ in dioxane) and AIBN (0.86 mg mL$^{-1}$ in dioxane) was prepared. This solution, *t*BA, and BA were transferred into different containers and placed inside the automated synthesizer. Aliquots of the prepared stock solution of CTA and AIBN, *t*BA, BA, and solvent were transferred from the containers into different reactors (100 mL) of the synthesizer with the automated liquid handling system to provide the desired concentration of reagents resulting in a final volume of 10 mL (please note that volume changes due to mixing of the reagents have been neglected). 1,3,5-Trioxane was added as internal standard at a concentration of 10 mg mL$^{-1}$ of total reaction volume. Each reactor was degassed in the parallel synthesizer by sparging with inert gas ($N_2$) for 15 min at 0 °C in parallel. Thereafter, the reaction mixtures were heated to 60 °C. Aliquots were taken periodically (4, 6, 8, and 11 h) for $^1$H NMR (0.075 mL) and SEC (0.05 mL) analysis under an inert gas flow. Once the desired molar masses were obtained, the polymerizations were stopped by decreasing the temperature to 10 °C. In order to avoid the high molar mass shoulder which occurs at very high monomer conversions, the conversions of *t*BA and BA were targeted to be 80% or less. Each reaction mixture was used directly for the chain extension without further purification.

**Second block:** Once the desired molar mass was obtained for the first block, the monomers remaining in the reaction mixtures were calculated based on the conversions. The amount of new monomers required were then calculated based on the remaining monomers and the targeted conversions. Thereafter, new monomers (*t*BA and BA) and initiators (AIBN, stock solution of 2 mg mL$^{-1}$ in dioxane) were added using the same method as described above. The new reaction mixtures were then degassed by sparging with inert gas ($N_2$) for 15 min at 0 °C. Thereafter, the reaction mixtures were heated to 60°C. During each polymerization, aliquots were taken periodically (2, 3, and 4 h) for $^1$H NMR (0.075 mL) and SEC (0.05 mL) analysis under an inert gas flow. Once the desired molar masses were obtained, the polymerizations were stopped by decreasing the temperature to 10 °C. After that, the reaction mixtures were removed from the reactors, diluted with methanol and twice precipitated in water/methanol (1/3, v/v) to remove all remaining monomers (checked by $^1$H NMR) and dried under vacuum. Full experimental details for each copolymer are given in Table S1 and SEC traces are shown in Figures S3 and S4.

**Table S1. Experimental conditions used for the synthesis and characterization data of the asymmetric diblock copolymers D10 and D20**

| | **D10**[a] | | | | **D20**[a] | | | |
|---|---|---|---|---|---|---|---|---|
| | 1st block | | 2nd block | | 1st block | | 2nd block | |
| $[\mathrm{Monomer}]_0$ (mol.L$^{-1}$) | tBA | BA | tBA | BA | tBA | BA | tBA | BA |
| | 3.36 | 0.64 | 0.48 | 2.52 | 3.36 | 0.64 | 0.48 | 2.52 |
| $[\mathrm{CTA}]_0/[\mathrm{AIBN}]_{\mathrm{added}}$ | 50 | | 30 | | 50 | | 32.5 | |
| $[\mathrm{AIBN}]_{\mathrm{added}}$ (mmol.L$^{-1}$) | 1.11 | | 1.11 | | 0.556 | | 0.556 | |
| $[\mathrm{Monomer}]_0/[\mathrm{CTA}]_0$ | 50.4 | 9.6 | 15.8 | 83.2 | 100.8 | 19.2 | 29.5 | 153.4 |
| $[\mathrm{m_{CTA}}]_{\mathrm{added}}$ (mg) | 211.7 | | 0 | | 105.8 | | 0 | |
| $[\mathrm{m_{monomer}}]_{\mathrm{added}}$ (g) | 4.31 | 0.820 | 0.544 | 6.32 | 4.31 | 0.820 | 0.208 | 5.78 |
| $[\mathrm{m_{AIBN}}]_{\mathrm{added}}$ (mg) | 1.8 | | 3.6 | | 0.9 | | 1.7 | |
| $[\mathrm{V_{dioxane}}]_{\mathrm{added}}$ (mL) | 2.04 | | 1.38 | | 3.10 | | 1.83 | |
| reaction time (h) | 11 | | 4 | | 11 | | 4 | |
| monomer conversion[b] | 82.5% | 82.5% | 42.5% | 47.0% | 76.1% | 76.7% | 38.1% | 38.0% |
| $[\mathrm{DP}]_{\mathrm{th}}$[c] | 41.6 | 7.9 | 6.7 | 39.1 | 76.7 | 14.7 | 11.2 | 58.3 |
| $M_{\mathrm{n,th}}$[d] (kg mol$^{-1}$) | 6.7 | | 12.5 | | 12.0 | | 20.9 | |
| $M_{\mathrm{n,SEC}}$[e] (kg mol$^{-1}$) | 4.9 | | 10.8 | | 10.0 | | 19.2 | |
| $Đ$[e] | 1.11 | | 1.09 | | 1.12 | | 1.10 | |

[a]Targeted molar mass [b]Determined by $^1$H NMR [c]$[\mathrm{DP}]_{\mathrm{th}} = [\mathrm{Monomer}]_0/[\mathrm{CTA}]_0 \times$ monomer conversion [d]$M_{\mathrm{n,th}} = [\mathrm{DP}]_{\mathrm{th}} \times M_{\mathrm{M}} + M_{\mathrm{CTA}}$, $M_{\mathrm{M}}$ and $M_{\mathrm{CTA}}$ are the molar mass of monomer and CTA respectively [e]Determined by SEC using $CHCl_3$ as an eluent with PMMA as molar mass standards (SEC system in IOMC, JCSM, Friedrich Schiller University Jena)

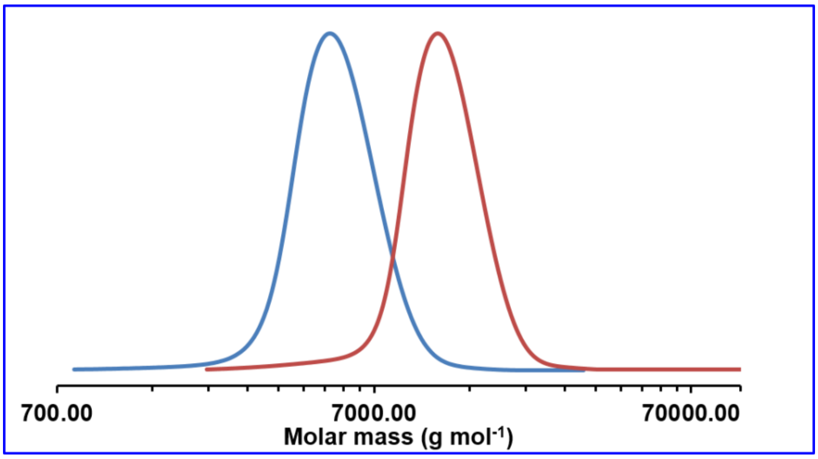

**Figure S3.** Molar mass distribution of each block (SEC RI traces in $CHCl_3$) for **D10**. Samples were analyzed in SEC system in IOMC, JCSM, Friedrich Schiller University Jena.

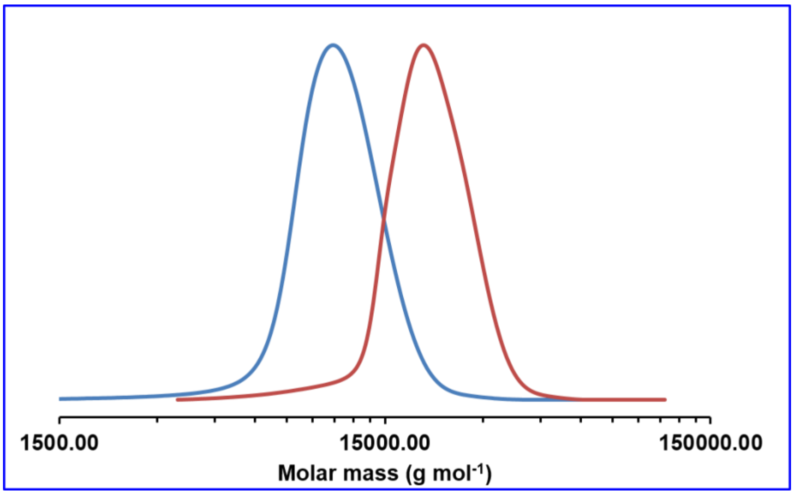

**Figure S4.** Molar mass distribution of each block (SEC RI traces in $CHCl_3$) for the asymmetric diblock copolymer **D20**. Samples were analyzed in SEC system in IOMC, JCSM, Friedrich Schiller University Jena.

***Synthesis of triblock copolymers (polytBA-b-poly(tBA$_{50\%}$-ran-BA$_{50\%}$)-b-polyBA, (T10 and T20).*** Copolymerizations were performed in a Chemspeed Accelerator SLT automated parallel synthesizer using a sequential reagent addition and similar experimental protocols as reported elsewhere.[S4-S7]

**First block:** Stock solutions of CTA (100 mg mL$^{-1}$ in dioxane) and AIBN (2 mg mL$^{-1}$ in dioxane) were prepared. These stock solutions and *t*BA were transferred into different containers and placed inside the automated synthesizer. Afterwards, for each investigated triblock polymer system, aliquots of the prepared stock solution of CTA, stock solution of AIBN, *t*BA, and solvent were transferred from the containers into different reactors (100 mL) of the synthesizer with the automated liquid handling system to provide the desired concentration of reagents resulting in a final volume of 13 mL (volume changes due to mixing of the reagents have been neglected). 1,3,5-Trioxane was added as internal standard at a concentration of 10 mg mL$^{-1}$ of total reaction volume. The reaction mixtures were degassed by sparging with inert gas ($N_2$) for 15 min at 0 °C. Thereafter, the reaction mixtures were heated to 60 °C. During each polymerization, aliquots were taken periodically (4, 6, and 8 h for 10 kg mol$^{-1}$ copolymer, and 4 and 8h for molar mass of 20 kg mol$^{-1}$ copolymer) for $^1$H NMR (0.075 mL) and SEC (0.05 mL) analysis under an inert gas flow. Once the desired molar masses were obtained, the polymerizations were stopped by decreasing the temperature to 10 °C. Each reaction mixture was used directly for the chain extension without further purification.

**Second block:** Once the desired molar masses were obtained for the first block, the remaining monomers in the reaction mixtures were calculated based on the conversions. The amount of new monomers required were calculated based on the remaining monomers and the targeted conversions. Thereafter, new monomers (*t*BA and BA) and initiators (AIBN, stock solution of 2 mg mL$^{-1}$ in dioxane) were added and the reaction mixtures degassed using the same method as described above. Thereafter, the reaction mixtures were heated to 60 °C. During each polymerization, aliquots were taken periodically (2 and 2.5 h) for $^1$H NMR (0.075 mL) and SEC (0.05 mL) analysis under an inert gas flow. Once the desired molar masses were obtained, the polymerizations were stopped by decreasing the temperature to 10 °C. After that, the reaction mixtures were removed from the reactors, diluted with methanol and precipitated twice in water/methanol (1/3, v/v) to remove all remaining monomers (checked by $^1$H NMR) and then dried under vacuum.

**Third block:** The obtained polymers from the last step were dissolved in dioxane and then transferred into different reactors (100 mL) of the synthesizer. The amount of BA required for the third block was calculated based on the amount of polymers added and the targeted conversions. Thereafter, BA and initiators (AIBN, stock solution of 2 mg mL$^{-1}$ in dioxane) were added and the reaction mixtures degassed using the same method as described above. Thereafter, the reaction mixtures were heated to 60 °C. During each polymerization, aliquots were taken periodically (2 and 3 h for molar mass of 10000 g mol$^{-1}$ copolymer, and 2, 3 and 3.5 h for molar mass of 20000 g mol$^{-1}$ copolymer) for $^1$H NMR (0.075 mL) and SEC (0.05 mL) analysis under an inert gas flow. Once the desired molar masses were obtained, the polymerizations were stopped by decreasing the temperature to 10 °C. After that, the reaction mixtures were removed from the reactors, diluted with methanol and twice precipitated in water/methanol (1/3, v/v) to remove all the remaining monomers (checked by $^1$H NMR) and then dried under vacuum. Full experimental details are given in Table S2 and SEC traces are shown in Figure S5 and S6.

**Table S2. Experimental conditions used for the synthesis and characterization data of the asymmetric triblock copolymers T10 and T20.**

| | T10 [a] | | | | T20[a] | | | |
|---|---|---|---|---|---|---|---|---|
| | 1st block | 2nd block | | 3rd block | 1st block | 2nd block | | 3rd block |
| $[\text{Monomer}]_0$ (mol.L$^{-1}$) | tBA | tBA | BA | BA | tBA | tBA | BA | BA |
| | 2.585 | 1.7 | 1.7 | 0.741 | 3.36 | 1.9 | 1.9 | 0.844 |
| $[\text{CTA}]_0/[\text{AIBN}]_{\text{added}}$ | 50 | 31.5 | | 12.5 | 50 | 33.1 | | 12.5 |
| $[\text{AIBN}]_{\text{added}}$ (mmol.L$^{-1}$) | 2.46 | 1.64 | | 2.28 | 1.33 | 0.89 | | 1.34 |
| $[\text{Monomer}]_0/[\text{CTA}]_0$ | 21 | 34.8 | 34.8 | 26 | 50.4 | 69.6 | 69.6 | 50.4 |
| $[\text{m}_{\text{CTA}}]_{\text{added}}$ (g) | 0.508 | 0 | | 2.81<br>(MacroCTA) | 0.212 | 0 | | 5.24<br>(MacroCTA) |
| $[\text{m}_{\text{monomer}}]_{\text{added}}$ (g) | 4.31 | 5.62 | 6.74 | 1.14 | 4.31 | 4.39 | 5.52 | 2.27 |
| $[\text{m}_{\text{AIBN}}]_{\text{added}}$ (mg) | 5.3 | 8.3 | | 4.5 | 2.2 | 3.3 | | 4.6 |
| $[\text{V}_{\text{dioxane}}]_{\text{added}}$ (mL) | 0.370 | 0.527 | | 0.1 | 1.867 | 0.541 | | 1.0 |
| reaction time (h) | 8 | 2.5 | | 3 | 8 | 2.5 | | 3.5 |
| monomer conversion[c] | 72.5% | 66.8% | 66.9% | 43.1% | 71.7% | 56.3% | 55.2% | 42.5% |
| $[\text{DP}]_{\text{th}}$[d] | 15.2 | 23.3 | 23.3 | 11.2 | 36.2 | 39.2 | 38.4 | 21.4 |
| $M_{\text{n,th}}$[e] (kg mol$^{-1}$) | 2.3 | 8.2 | | 9.7 | 5.0 | 14.9 | | 17.6 |
| $M_{\text{n,SEC}}$[f] (kg mol$^{-1}$) | 1.7 | 7.8 | | 10.0 | 4.1 | 15.9 | | 20.1 |
| *Đ*[f] | 1.10 | 1.08 | | 1.07 | 1.09 | 1.07 | | 1.07 |

[a]Targeted molar mass [b]Determined by $^1$H NMR [c]$[\text{DP}]_{\text{th}} = [\text{Monomer}]_0/[\text{CTA}]_0 \times$ monomer conversion [d]$M_{\text{n,th}} = [\text{DP}]_{\text{th}} \times M_{\text{M}} + M_{\text{CTA}}$, $M_{\text{M}}$ and $M_{\text{CTA}}$ are the molar mass of monomer and CTA respectively [e]Determined by SEC using $CHCl_3$ as an eluent with PMMA as molar mass standards (SEC system in IOMC, JCSM, Friedrich Schiller University Jena)

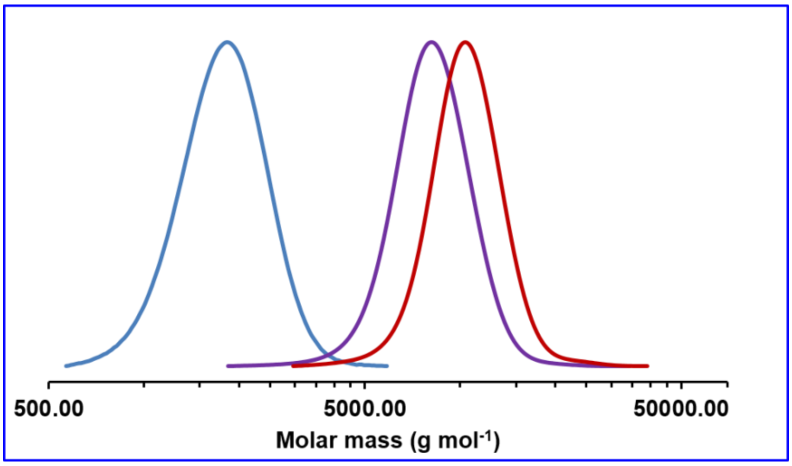

**Figure S5.** Molar mass distribution of each block (SEC RI traces in $CHCl_3$) for the asymmetric triblock copolymer **T10**. Samples were analyzed in SEC system in IOMC, JCSM, Friedrich Schiller University Jena.

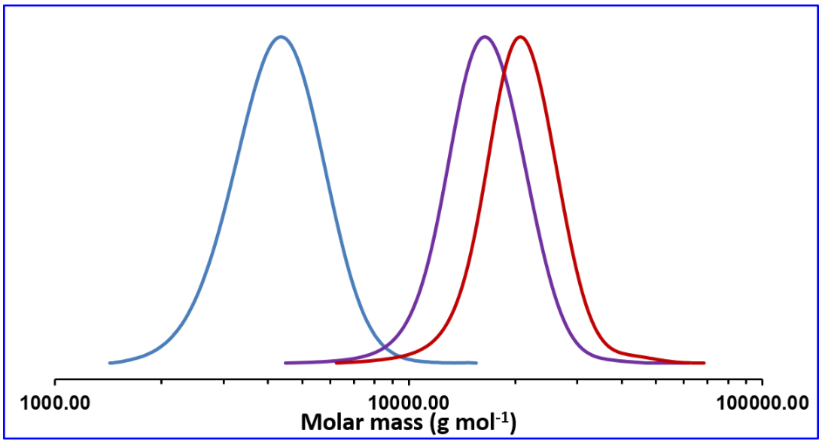

**Figure S6.** Molar mass distribution of each block (SEC RI traces in $CHCl_3$) for the asymmetric triblock copolymer **T20**. Samples were analyzed in SEC system in IOMC, JCSM, Friedrich Schiller University Jena.

### *Synthesis of gradient copolymers (poly($BA_{50\%}$-grad-t$BA_{50\%}$) (G10 and G20).*

Gradient copolymerizations were performed at 90°C with ACHN as a thermal initiator. An initial solution of CTA and ACHN in anisole was prepared and degassed by sparging with Ar for 30 minutes. Degassed pure *t*BA (7.90 g, 9.0 mL, 61.6 mmol) and BA (4.50g, 5.0 mL, 35 mmol) were added into the reaction mixture via syringe pumps at a total addition rate of 1.75 $mL.h^{-1}$. At the beginning of the polymerization, 0.875 mL of BA was added in one shot to the reactor. Thereafter, the addition rate of each monomer was adjusted so that the rate of tBA addition increased linearly from 0 to 1.75 $mL.h^{-1}$ over 6h, and on the contrary the rate of BA decreased linearly from 1.75 to 0 $mL.h^{-1}$ within 6h. At the final stage of the reaction, 2.63 mL of *t*BA were added during 3 h at 1.75 $mL.h^{-1}$. The addition program is shown in Figures S7 and S8 for **G10** and **G20**, respectively. Aliquots of the reaction mixture were taken periodically and analyzed with $^1H$ NMR and SEC to determine the reaction mixture composition and macromolecular characteristics of the polymer formed (Figures S7 and S8 for **G10** and **G20**, respectively). After 10h (**G10**) or 7.5 h (**G20**), the reaction mixture was concentrated under vacuum to remove unreacted monomer, precipitated in 10% water in methanol and dried under deep vacuum. The final composition of **G10** was 51.4% BA, 48.6% *t*BA, and that of **G20** was 43.9% BA, 56.1% *t*BA. The molar mass and dispersities were **G10**: $M_n$ = 8.0 kg $mol^{-1}$, $Đ$ = 1.38; and **G20**: $M_n$ = 28.9 kg $mol^{-1}$, $Đ$ = 1.35.

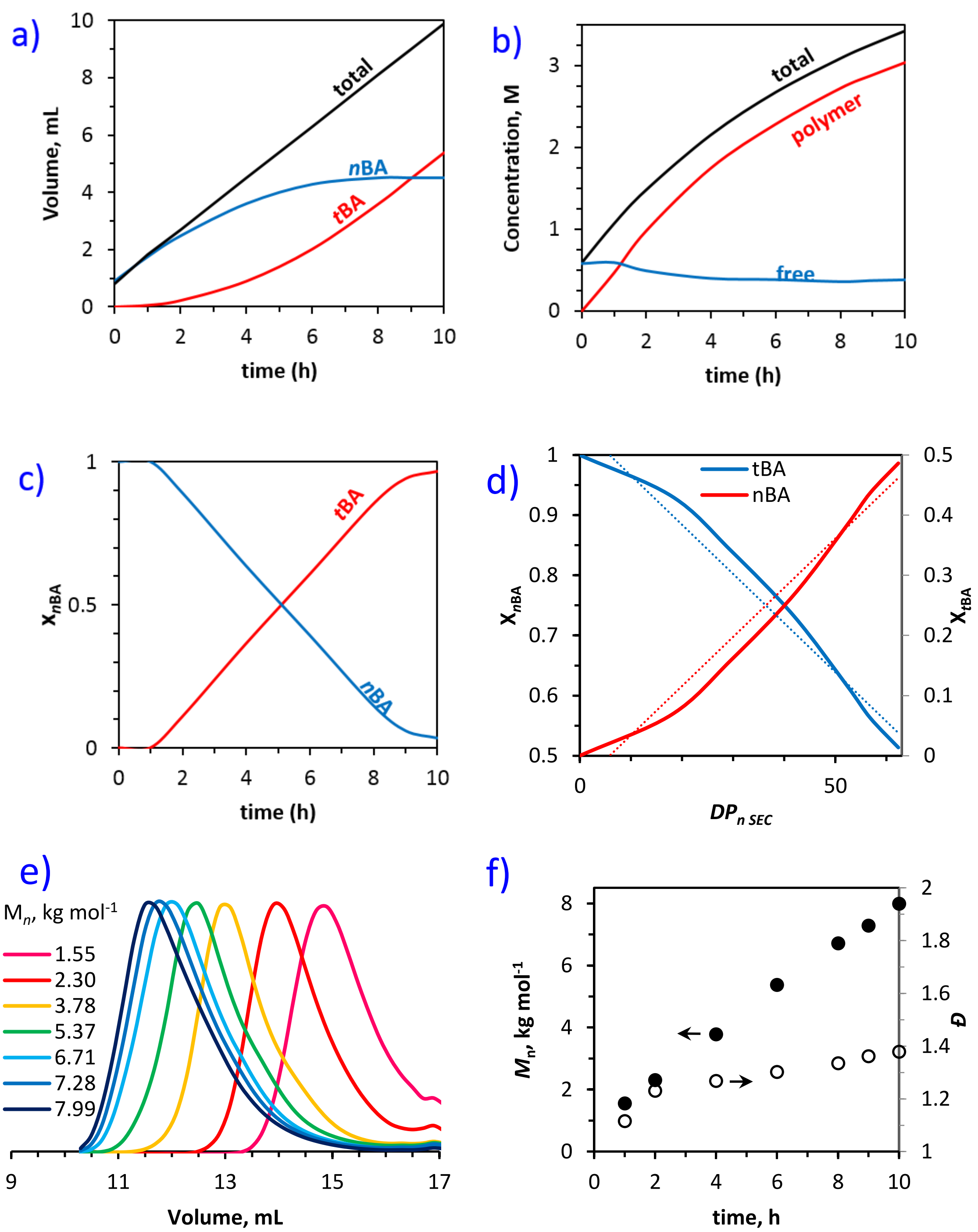

**Figure S7.** Data for the gradient copolymer **G10**: a) monomer addition program for the synthesis; b) composition of the reaction mixture over the course of the polymerization (molar concentration of BA units in both monomer and polymer); c) composition of the free monomer mixture over the course of the polymerization; d) cumulative polymer composition of the gradient copolymer: final composition 51.4% BA, 48.6% *t*BA; e) SEC trace evolution over the course of the polymerization (samples were analyzed in SEC system in Laboratoire des IMRCP, Université de Toulouse); f) evolution of $M_n$ and $Đ$ over the course of the polymerization: final $M_{n,\mathrm{SEC}}$ = 8.0 kg mol$^{-1}$, $Đ$ = 1.38.

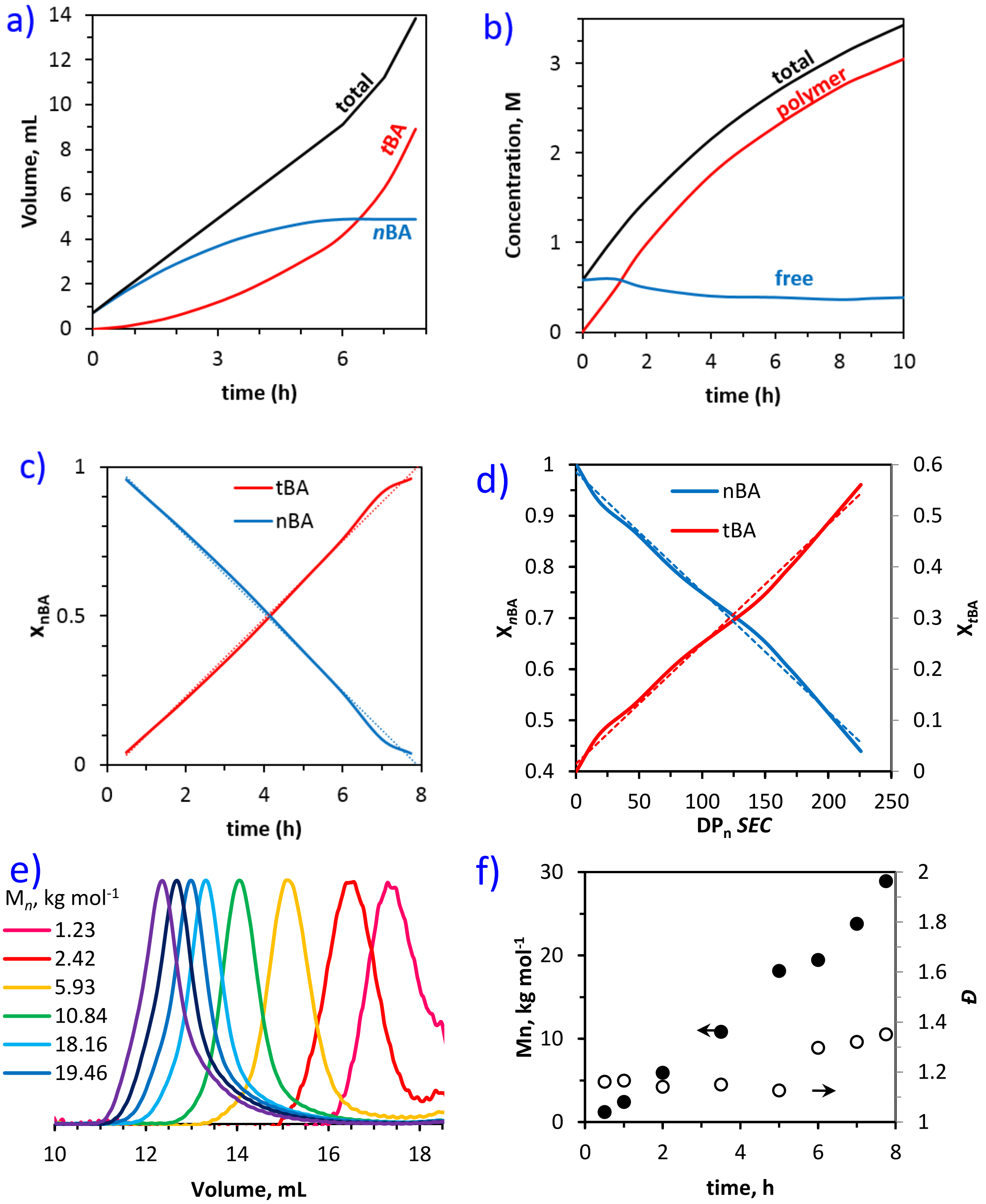

**Figure S8.** Data for the gradient copolymer **G20**: a) monomer addition program for the synthesis; b) composition of the reaction mixture over the course of the polymerization (molar concentration of BA units in both monomer and polymer); c) composition of the free monomer mixture over the course of the polymerization; d) cumulative polymer composition of the copolymer: final composition 43.9% BA, 56.1% *t*BA; e) SEC traces evolution over the course of the polymerization (samples were analyzed in SEC system in Laboratoire des IMRCP, Université de Toulouse); f) evolution of $M_n$ and $Đ$ over the course of the polymerization: final $M_{n,SEC}$ = 28.9 kg mol$^{-1}$, $Đ$ = 1.35.

### *Acidolysis of Polymers.*

Each polymer was first dissolved in 5 mL of DCM, then 5-fold excess (mol% corresponding to the amount (mol) of tBA units) of TFA was added at once. Reaction mixture was stirred at room temperature for 72 hours, rotary evaporated, dissolved in 10 mL of 1,4-dioxane and rotary evaporated again, washed with 10 mL of deionized water and dried under deep vacuum. $^1$H NMR analysis showed complete removal of tert-butyl groups.

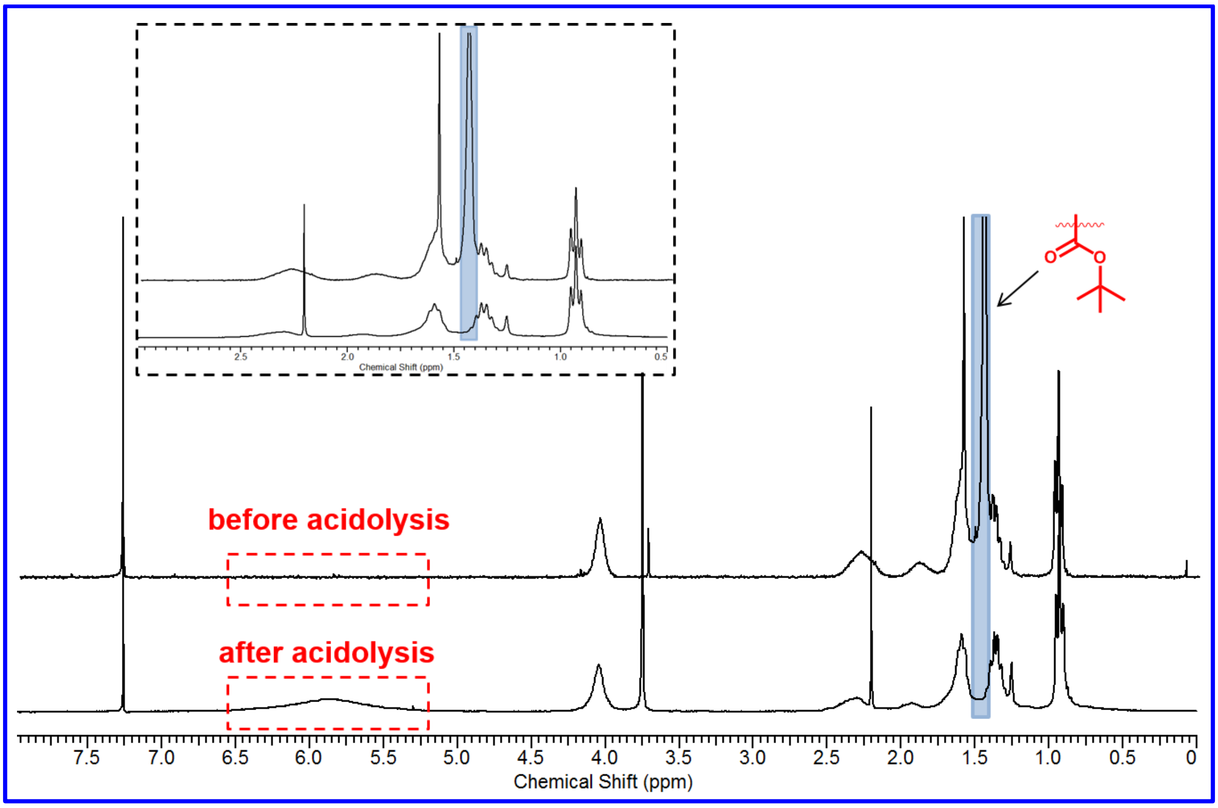

**Figure S9** The comparison of $^1$H NMR spectra ($CDCl_3$, 300MHz) of asymmetric diblock copolymer **D10** before acidolysis (top) and after acidolysis (bottom). The inset is a zoomed in image of the chemical shift between 0.5 and 3 ppm. The gray parts show that the tertbutyl group (–C(C***H*<sub></sub>**$_3$)$_3$) disappears after acidolysis and a new carboxylic group (–COO***H***) appears (at around 5.8 ppm).

## 5. POTENTIOMETRIC TITRATIONS

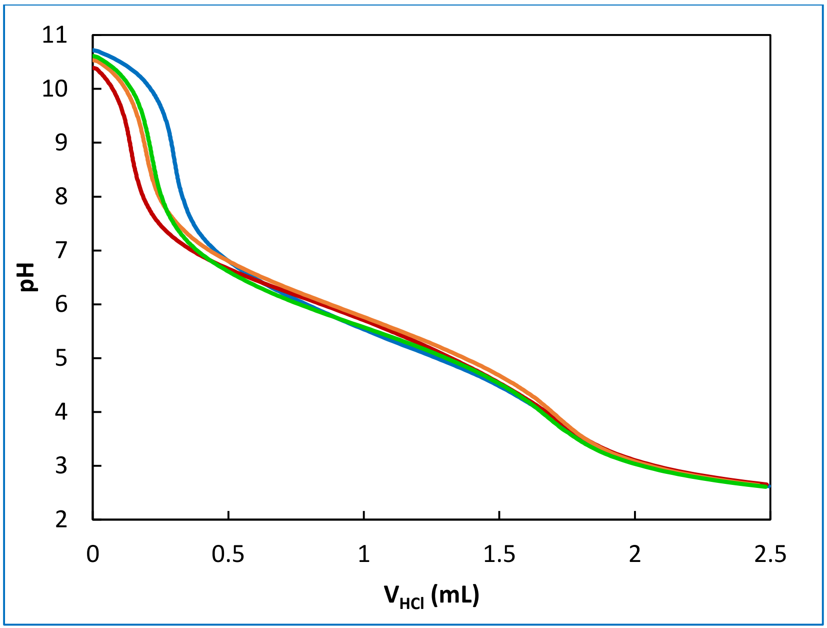

**Figure S10**. Raw potentiometric titration curves of block (—), diblock (—), triblock (—) and gradient (—) copolymers of 20 000 g.mol$^{-1}$. The solutions were titrated with HCl 0.1 M at a polymer concentration of 1 g.L$^{-1}$, with 0.1 M NaCl and starting with ~10% excess of NaOH.

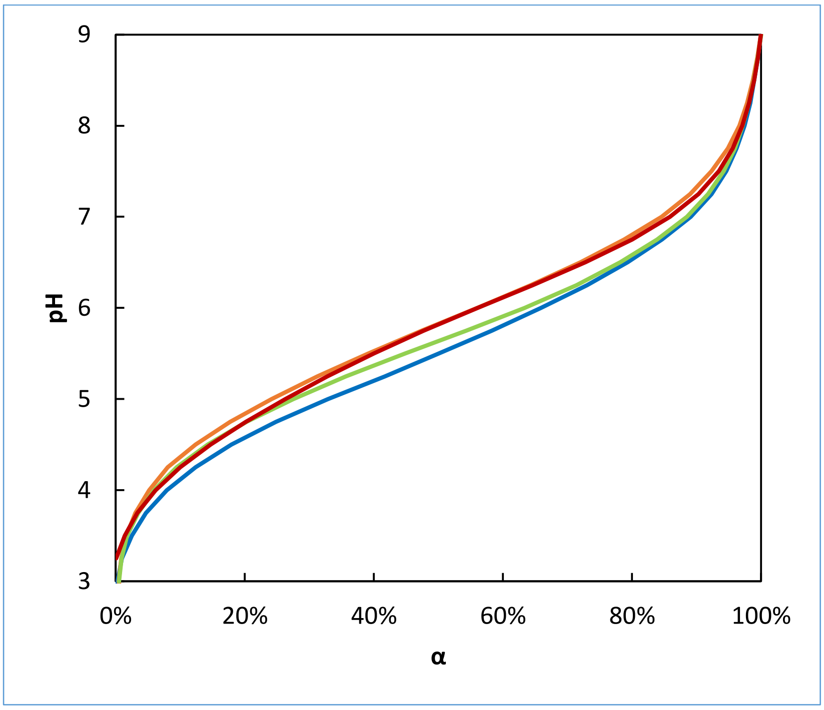

**Figure S11.** Comparison of pH as a function of ionization degree α for block (—), diblock (—), triblock (—) and gradient (—) copolymers of 20 000 g.mol$^{-1}$. The titrations were conducted from $\alpha = 1$ to $\alpha = 0$ with HCl 0.1 M at a polymer concentration of 1 g.L$^{-1}$ and with 0.1 M NaCl.

## 6. DYNAMIC LIGHT SCATTERING

### *6a. DLS pH Titration Study*

Solutions containing 0.2% weight of each polymer were prepared by dissolving them into a 0.1 M NaOH aqueous solution separately. The polymer solutions were filtered through a Nylon 66 membrane with 0.45 μm pore size before the titration study and were not filtered during the titration study. Each polymer solution was first titrated with an HCl solution (6 M and 1M) to lower the pH until the solution became cloudy. The same solution was then titrated with a NaOH solution (1 M and 0.1 M) to increase the pH value. As the HCl or NaOH solution concentrations were relatively high, only a small amount of HCl or NaOH solution was needed to change the pH value. Therefore, the concentration of the polymer stayed relatively constant during the titration. The hydrodynamic diameters ($D_h$) and size distributions were determined using DLS as demonstrated above.

## Block copolymers B10 and B20

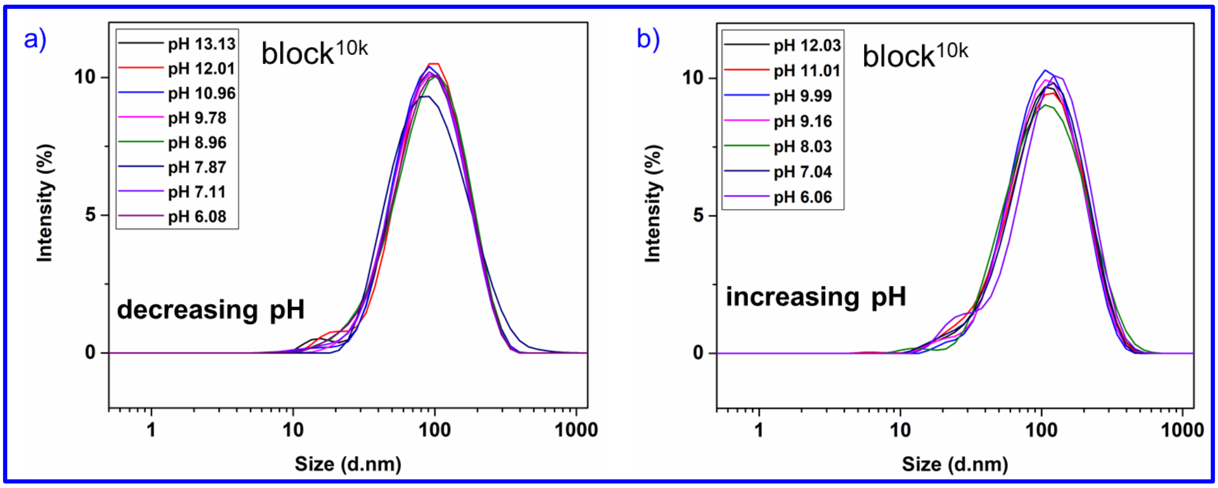

**Figure S12.** Apparent size distributions obtained by DLS for the titration study of **B10** (poly(BA$_{50\%}$-*block*-AA$_{50\%}$) with molar mass of 10 kg mol$^{-1}$): a) decreasing the pH value by adding HCl solution; b) increasing the pH value by adding NaOH solution.

**Table S3.** Characterization data of the titration study for **B10** by DLS.

| **B10** | Decreasing pH value[a] | **13.1** | **12.0** | **11.0** | **9.8** | **9.0** | **7.9** | **7.1** | **6.1** |
|---|---|---|---|---|---|---|---|---|---|
| | $D_h$ (nm)[c] | 78 | 79 | 78 | 78 | 78 | 78 | 77 | 77 |
| | PDI[d] | 0.25 | 0.24 | 0.24 | 0.24 | 0.25 | 0.24 | 0.24 | 0.24 |
| | Increasing pH value[b] | **6.1** | **7.0** | **8.0** | **9.2** | **10.0** | **11.0** | **12.0** | |
| | $D_h$ (nm)[c] | 94 | 90 | 89 | 88 | 87 | 87 | 87 | |
| | PDI[d] | 0.27 | 0.27 | 0.26 | 0.26 | 0.25 | 0.27 | 0.27 | |

[a] The pH value was decreased by adding HCl solution to the polymer solution. [b] The pH value was increased by adding NaOH solution to the polymer solution. [c] The apparent Z-average hydrodynamic diameter of the nanoparticles. [d] Apparent polydispersity index of the nanoparticles.

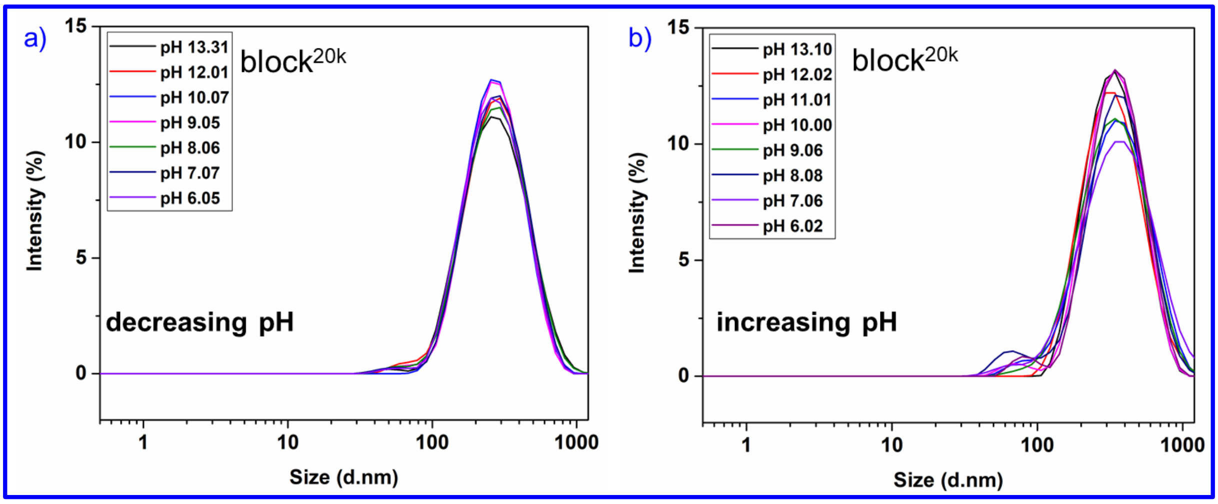

**Figure S13.** Apparent size distributions obtained by DLS for the titration study of block copolymer **B20**: a) decreasing the pH value by adding HCl solution; b) increasing the pH value by adding NaOH solution.

**Table S4.** Characterization data of the titration study for B20 by DLS.

| | | | | | | | | | |
|---|---|---|---|---|---|---|---|---|---|
| | Decreasing pH value[a] | **13.3** | **12.0** | **10.1** | **9.1** | **8.1** | **7.1** | **6.1** | |
| | $D_h$ (nm)[c] | 230 | 226 | 227 | 226 | 227 | 227 | 224 | |
| | PDI[d] | 0.25 | 0.25 | 0.23 | 0.24 | 0.25 | 0.25 | 0.24 | |
| **B20** | Increasing pH value[b] | **6.0** | **7.1** | **8.1** | **9.1** | **10.0** | **11.0** | **12.0** | **13.1** |
| | $D_h$ (nm)[c] | 284 | 284 | 277 | 273 | 270 | 273 | 266 | 265 |
| | PDI[d] | 0.26 | 0.29 | 0.27 | 0.26 | 0.26 | 0.28 | 0.25 | 0.25 |

[a] The pH value was decreased by adding HCl solution to the polymer solution. [b] The pH value was increased by adding NaOH solution to the polymer solution. [c] The apparent Z-average hydrodynamic diameter of the nanoparticles. [d] Apparent polydispersity index of the nanoparticles.

### Asymmetric Diblock Copolymers D10 and D20

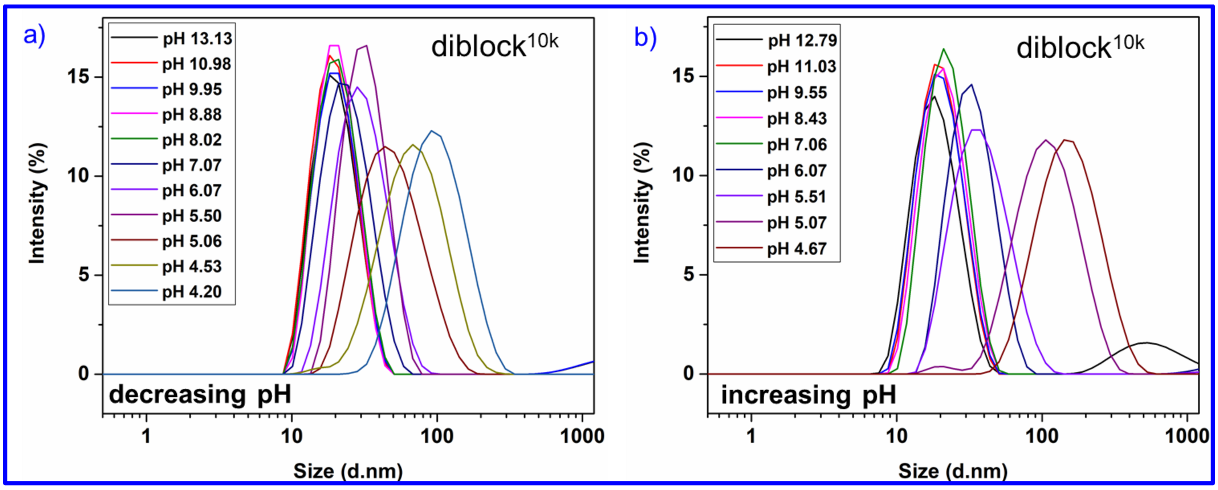

**Figure S14.** Apparent size distributions obtained by DLS for the titration study of the asymmetric diblock copolymer **D10** (10 kg mol$^{-1}$): a) decreasing the pH value by adding HCl solution; b) increasing the pH value by adding NaOH solution. The low intensity, large diameter (≥200 nm) populations observed at pH value 9.95 (decreasing pH value) and pH value 6.07 (increasing pH value) are most probably either due to contamination by dust particles or to a negligible weight fraction of spurious aggregates[S8,S9] as no corresponding structures were observed in cryoTEM and these populations are not seen at slightly higher or lower pH value.

**Table S5.** Characterization data of the titration study for **D10** using DLS.

| | | | | | | | | | | | | |
|---|---|---|---|---|---|---|---|---|---|---|---|---|
| **D10** | Decreasing pH value[a] | **13.1** | **11.0** | **10.0** | **8.9** | **8.0** | **7.1** | **6.1** | **5.5** | **5.1** | **4.5** | **4.2** |
| | $D_h$ (nm)[c] | 21 | 20 | 21 | 21 | 21 | 23 | 28 | 30 | 43 | 60 | 87 |
| | PDI[d] | 0.25 | 0.21 | 0.25 | 0.22 | 0.21 | 0.18 | 0.14 | 0.09 | 0.18 | 0.18 | 0.16 |
| | Increasing pH value[b] | **4.7** | **5.1** | **5.5** | **6.1** | **7.1** | **8.4** | **9.6** | **11.0** | **12.8** | | |
| | $D_h$ (nm)[c] | 132 | 93 | 37 | 34 | 22 | 21 | 20 | 20 | 20 | | |
| | PDI[d] | 0.19 | 0.21 | 0.23 | 0.24 | 0.21 | 0.22 | 0.21 | 0.21 | 0.28 | | |

[a] The pH value was decreased by adding HCl solution to the polymer solution. [b] The pH value was increased by adding NaOH solution to the polymer solution. [c] The apparent Z-average hydrodynamic diameter of the nanoparticles. [d] Apparent polydispersity index of the nanoparticles.

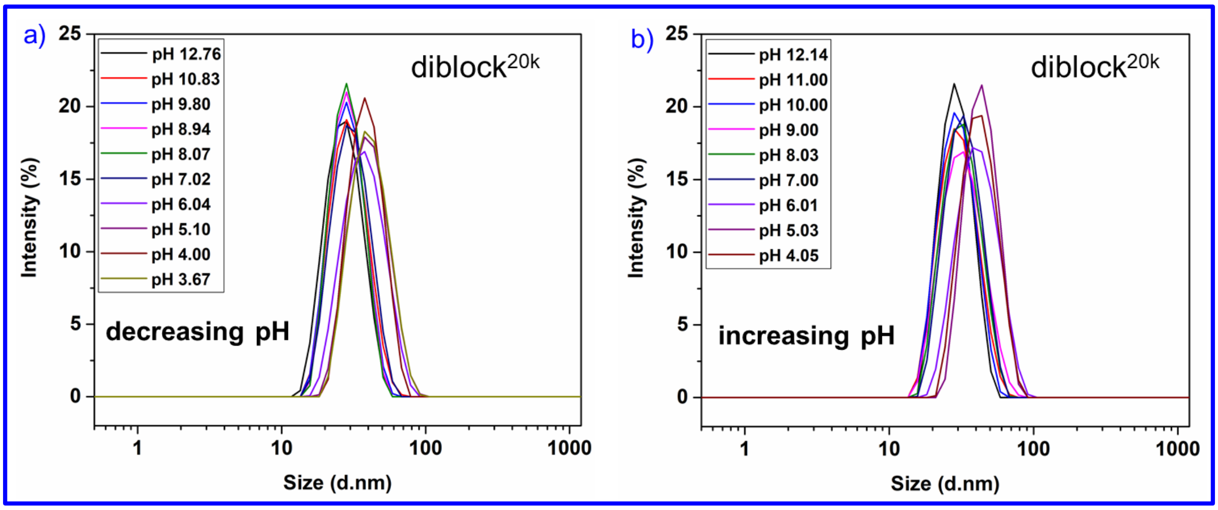

**Figure S15.** Apparent size distributions obtained by DLS for the titration study of the asymmetric diblock copolymer **D20** (20 kg mol$^{-1}$): a) decreasing the pH value by adding HCl solution; b) increasing the pH value by adding NaOH solution.

**Table S6.** Characterization data of the titration study for D20 using DLS.

| | | | | | | | | | | | |
|---|---|---|---|---|---|---|---|---|---|---|---|
| **D20** | Decreasing pH value[a] | **12.8** | **10.8** | **9.8** | **8.9** | **8.1** | **7.0** | **6.0** | **5.1** | **4.0** | **3.7** |
| | $D_h$ (nm)[c] | 26 | 28 | 28 | 28 | 28 | 29 | 35 | 38 | 37 | 39 |
| | PDI[d] | 0.06 | 0.07 | 0.06 | 0.05 | 0.04 | 0.06 | 0.08 | 0.08 | 0.05 | 0.09 |
| | Increasing pH value[b] | **4.1** | **5.0** | **6.0** | **7.0** | **8.0** | **9.0** | **10.0** | **11.0** | **12.1** | |
| | $D_h$ (nm)[c] | 40 | 42 | 39 | 31 | 30 | 31 | 28 | 29 | 28 | |
| | PDI[d] | 0.06 | 0.04 | 0.08 | 0.07 | 0.08 | 0.11 | 0.07 | 0.08 | 0.04 | |

[a] The pH value was decreased by adding HCl solution to the polymer solution. [b] The pH value was increased by adding NaOH solution to the polymer solution. [c] Apparent Z-average hydrodynamic diameter of the nanoparticles. [d] Apparent polydispersity index of the nanoparticles.

## Asymmetric Triblock Copolymers T10 and T20

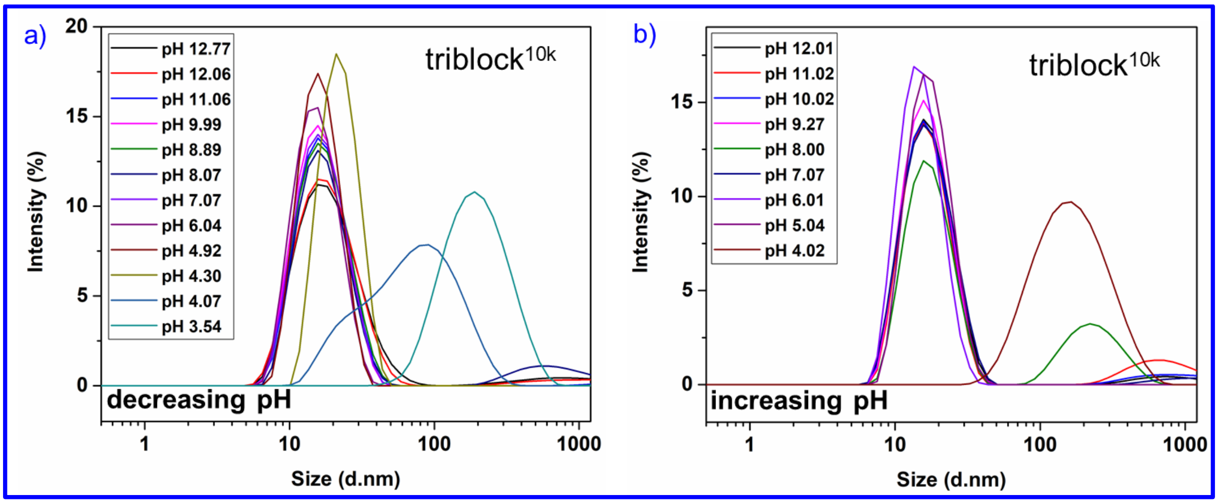

**Figure S16.** Apparent size distributions obtained by DLS for the titration study of the asymmetric triblock copolymer **T10** (10 kg mol$^{-1}$): a) decreasing the pH value by adding HCl solution; b) increasing the pH value by adding NaOH solution. The low intensity, large diameter (≥200 nm) populations observed at pH value > 11 (decreasing pH value) and pH value > 10 and pH value 8 (increasing pH value) are most probably either due to contamination by dust particles or to a negligible weight fraction of spurious aggregates[S8,S9] as no corresponding structures were observed in cryoTEM. The bimodal distribution observed at pH value 4.07 (decreasing pH value) suggests the presence of a mixture of small and large aggregates. Similar distributions were observed in DLS of **T20** and **G10** (see Figures S17, S18) Due to the limitations of the fitting algorithm when applied to bimodal distributions, the distribution shown may not be an accurate representation of the true size distribution.

**Table S7.** Characterization data of the titration study for **T10** (10 kg mol$^{-1}$) using DLS.

| | Decreasing pH value[a] | **12.8** | **12.1** | **11.1** | **10.0** | **8.9** | **8.1** | **7.1** | **6.0** | **4.9** | **4.3** | **4.1** | **3.5** |
|---|---|---|---|---|---|---|---|---|---|---|---|---|---|
| | $D_h$ (nm)[c] | 18 | 17 | 17 | 15 | 16 | 18 | 16 | 15 | 15 | 21 | 54 | 178 |
| | PDI[d] | 0.26 | 0.25 | 0.22 | 0.15 | 0.20 | 0.28 | 0.20 | 0.16 | 0.09 | 0.08 | 0.29 | 0.23 |
| **T10** | Increasing pH value[b] | **4.0** | **5.0** | **6.0** | **7.1** | **8.0** | **9.3** | **10.0** | **11.0** | **12.0** | | | |
| | $D_h$ (nm)[c] | 129 | 16 | 15 | 17 | 21 | 16 | 17 | 18 | 17 | | | |
| | PDI[d] | 0.28 | 0.12 | 0.15 | 0.21 | 0.37 | 0.20 | 0.25 | 0.27 | 0.22 | | | |

[a] The pH value was decreased by adding HCl solution to the polymer solution. [b] The pH value was increased by adding NaOH solution to the polymer solution. [c] Apparent Z-average hydrodynamic diameter of the nanoparticles. [d] Apparent polydispersity index of the nanoparticles.

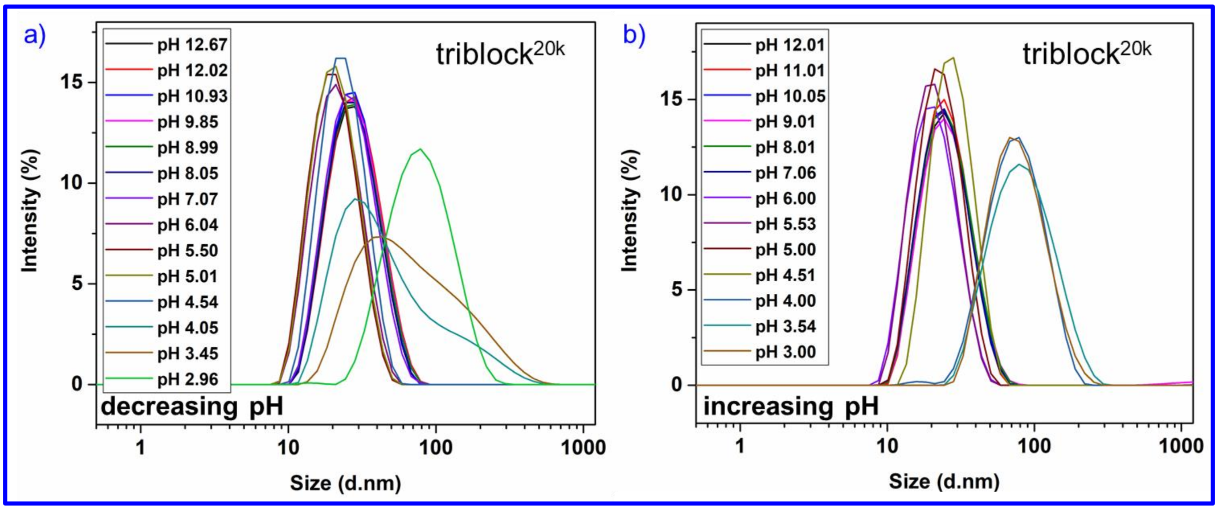

**Figure S17.** Apparent size distributions obtained by DLS for the titration study of the asymmetric triblock copolymer **T20** (20 kg mol$^{-1}$): a) decreasing the pH value by adding HCl solution; b) increasing the pH value by adding NaOH solution. The bimodal distributions observed at pH value 4.05 and 3.45 (decreasing pH value) may represent a mixture of small and large aggregates. Similar distributions were observed in DLS of **T10** and **G10** (see Figures S16, S18) Due to the limitations of the fitting algorithm when applied to bimodal distributions, the distribution shown may not be an accurate representation of the true size distribution.

**Table S8.** Characterization data of the titration study for **T20** using DLS.

| | Decreasing pH value[a] | **12.7** | **12.0** | **10.9** | **9.9** | **9.0** | **8.1** | **7.1** | **6.0** | **5.5** | **5.0** | **4.5** | **4.1** | **3.5** | **3.0** |
|---|---|---|---|---|---|---|---|---|---|---|---|---|---|---|---|
| **T20** | $D_h$ (nm) [c] | 27 | 26 | 26 | 26 | 26 | 27 | 26 | 21 | 20 | 20 | 22 | 37 | 52 | 70 |
| | PDI[d] | 0.19 | 0.14 | 0.14 | 0.14 | 0.15 | 0.20 | 0.18 | 0.18 | 0.15 | 0.12 | 0.11 | 0.27 | 0.35 | 0.17 |
| | Increasing pH value[b] | **3.00** | **3.54** | **4.00** | **4.51** | **5.00** | **5.53** | **6.00** | **7.06** | **8.01** | **9.01** | **10.05** | **11.01** | **12.01** | |
| | $D_h$ (nm)[c] | 72 | 75 | 67 | 26 | 22 | 20 | 20 | 24 | 24 | 25 | 24 | 24 | 25 | |
| | PDI[d] | 0.17 | 0.16 | 0.15 | 0.10 | 0.10 | 0.14 | 0.21 | 0.19 | 0.16 | 0.22 | 0.18 | 0.18 | 0.21 | |

[a] The pH value was decreased by adding HCl solution to the polymer solution. [b] The pH value was increased by adding NaOH solution to the polymer solution. [c] Apparent Z-average hydrodynamic diameter of the nanoparticles. [d] Apparent polydispersity index of the nanoparticles.

## Gradient Copolymers G10 and G20

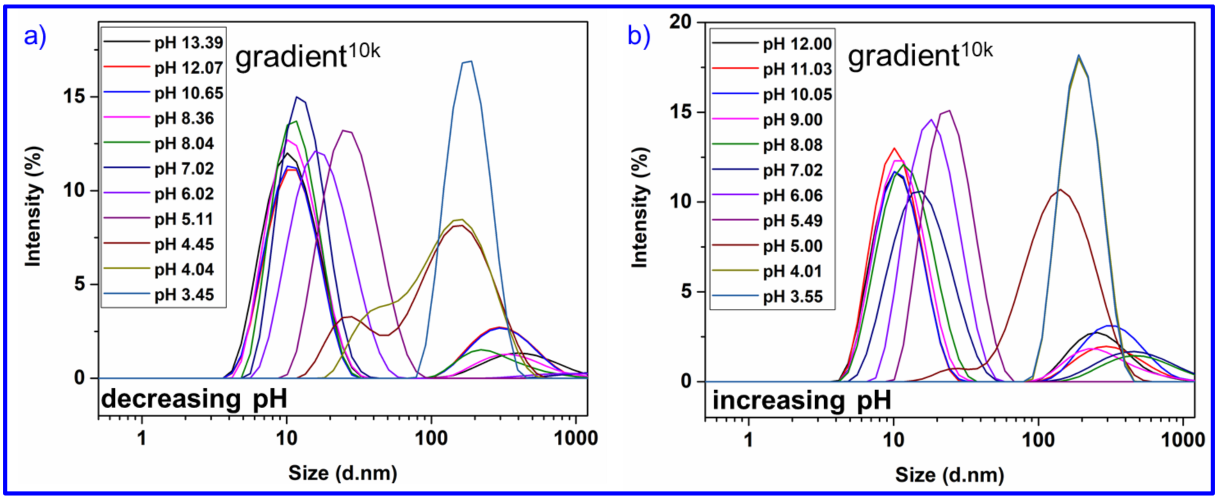

**Figure S18.** Apparent size distributions obtained by DLS for the titration study of gradient copolymer **G10**: a) decreasing the pH value by adding HCl solution; b) increasing the pH value by adding NaOH solution. The low intensity, large diameter (≥200 nm) populations observed at pH value > 7 are most probably either due to contamination by dust particles or to a negligible weight fraction of spurious aggregates[S8,S9] as no corresponding structures were observed in cryoTEM. The bimodal distributions observed at pH value 4-5 may represent a mixture of small and large aggregates. Similar distributions were observed in DLS of **T10** and **T20** (see Figures S16, S17) Due to the limitations of the fitting algorithm when applied to bimodal distributions, the distribution shown may not be an accurate representation of the true size distribution.

**Table S9.** Characterization data of the titration study for **G10** by DLS.

| | | | | | | | | | | | | |
|---|---|---|---|---|---|---|---|---|---|---|---|---|
| **G10** | Decreasing pH value[a] | **13.39** | **12.07** | **10.65** | **8.36** | **8.04** | **7.02** | **6.02** | **5.11** | **4.45** | **4.04** | **3.45** |
| | $D_h$ (nm)[c] | 11.3 | 13.4 | 13.1 | 11.9 | 13.3 | 12.9 | 16.6 | 25.5 | 80.0 | 93.4 | 171.6 |
| | PDI[d] | 0.29 | 0.40 | 0.38 | 0.29 | 0.35 | 0.21 | 0.21 | 0.15 | 0.46 | 0.30 | 0.08 |
| | Increasing pH value[b] | **3.55** | **4.01** | **5.00** | **5.49** | **6.06** | **7.02** | **8.08** | **9.00** | **10.05** | **11.03** | **12.00** |
| | $D_h$ (nm)[c] | 187 | 188.4 | 112.4 | 22.7 | 17.4 | 16.9 | 13.0 | 13.2 | 13.8 | 12.1 | 13.3 |
| | PDI[d] | 0.07 | 0.07 | 0.25 | 0.11 | 0.12 | 0.34 | 0.30 | 0.37 | 0.43 | 0.31 | 0.42 |

[a] The pH value was decreased by adding HCl solution to the polymer solution. [b] The pH value was increased by adding NaOH solution to the polymer solution. [c] Apparent Z-average hydrodynamic diameter of the nanoparticles. [d] Apparent polydispersity index of the nanoparticles.

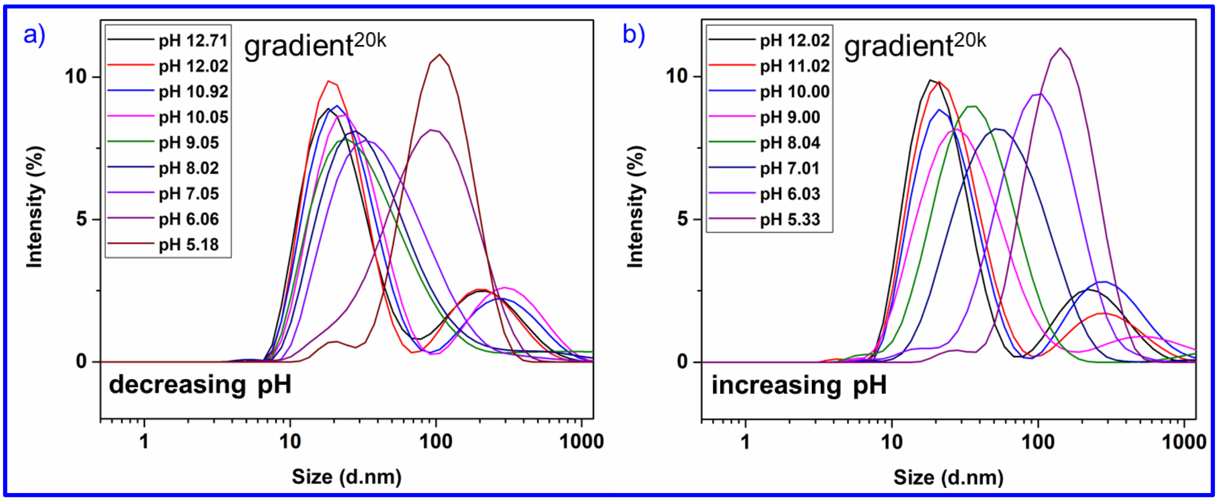

**Figure S19.** Apparent size distributions obtained by DLS for the titration study of gradient copolymer **G20**: a) decreasing the pH value by adding HCl solution and b) increasing the pH value by adding NaOH solution. The low intensity, large diameter (≥200 nm) populations observed at pH value > 10 (decreasing pH value) and pH value > 9 (increasing pH value) are most probably either due to contamination by dust particles or to a negligible weight fraction of spurious aggregates[S8,S9] as no corresponding structures were observed in cryoTEM.

**Table S10.** Characterization data of the titration study for **G20** by DLS.

| | | | | | | | | | | |
|---|---|---|---|---|---|---|---|---|---|---|
| **G20** | Decreasing pH value[a] | **12.71** | **12.02** | **10.92** | **10.05** | **9.05** | **8.02** | **7.05** | **6.06** | **5.18** |
| | $D_h$ (nm)[c] | 24.0 | 23.7 | 25.4 | 29.0 | 27.7 | 30.1 | 35.1 | 68.0 | 94.1 |
| | PDI[d] | 0.39 | 0.37 | 0.37 | 0.39 | 0.35 | 0.34 | 0.30 | 0.32 | 0.29 |
| | Increasing pH value[b] | **5.33** | **6.03** | **7.01** | **8.04** | **9.00** | **10.00** | **11.02** | **12.02** | |
| | $D_h$ (nm)[c] | 114.1 | 79.3 | 47.6 | 33.6 | 28.5 | 28.7 | 24.3 | 23.9 | |
| | PDI[d] | 0.26 | 0.27 | 0.28 | 0.29 | 0.36 | 0.40 | 0.34 | 0.37 | |

[b] The pH value was decreased by adding HCl solution to the polymer solution. [c] The pH value was increased by adding NaOH solution to the polymer solution. [d] Apparent Z-average hydrodynamic diameter. [e] Apparent polydispersity index.

### *6b. DLS study of polymer dispersions prepared by direct dispersion into buffers*

A 0.2 wt. % solution of the polymers was prepared by dispersing each polymer sample in pH buffers (0.1 M pH 10, 8, 7, 6, 5, and 4). The pH 10 buffer (0.1 M) was made using $Na_2CO_3$ and $NaHCO_3$. The pH 8, 7, and 6 buffers (0.1 M) were made using $NaH_2PO_4$ and $Na_2HPO_4$. The pH 5 and 4 buffers (0.1 M) were made using sodium acetate and acetic acid. As the polymers could not be dissolved in pH 4 buffer at room temperature, the dispersions at pH 4 were prepared by heating to 100 or 120 °C using a microwave reactor. The polymer solutions were filtered through a Nylon 66 membrane with 0.45 μm pore size before being analyzed by DLS.

**Table S11.** Characterization data of the nano-objects formed by the self-assembly of different types of copolymers directly dispersed in different pH buffers using DLS.

| **Sample**[a] | | **pH value** | | | | | |
|---|---|---|---|---|---|---|---|
| | | **10** | **8** | **7** | **6** | **5** | **4** |
| **B10** | $D_h$ (nm)[b] | 80 | 103 | 87 | 95 | precipitated | precipitated |
| | PDI[c] | 0.25 | 0.26 | 0.23 | 0.24 | - | - |
| **B20** | $D_h$ (nm)[b] | 291 | 280 | 269 | 279 | precipitated | precipitated |
| | PDI[c] | 0.29 | 0.28 | 0.34 | 0.26 | - | - |
| **D10** | $D_h$ (nm)[b] | 23 | 24 | 27 | 31 | 35 | 198 |
| | PDI[c] | 0.26 | 0.14 | 0.09 | 0.06 | 0.15 | 0.12 |
| **D20** | $D_h$ (nm)[b] | 31 | 37 | 43 | 47 | 47 | 191 |
| | PDI[c] | 0.04 | 0.03 | 0.03 | 0.02 | 0.01 | 0.22 |
| **T10** | $D_h$ (nm)[b] | 16 | 16 | 15 | 16 | 18 | 241 |
| | PDI[c] | 0.19 | 0.19 | 0.12 | 0.13 | 0.04 | 0.18 |
| **T20** | $D_h$ (nm)[b] | 25 | 25 | 23 | 21 | 25 | 167 |
| | PDI[c] | 0.16 | 0.17 | 0.19 | 0.12 | 0.04 | 0.22 |
| **G10** | $D_h$ (nm)[b] | 11 | 15 | 16 | 20 | 123 | 163 |
| | PDI[c] | 0.13 | 0.20 | 0.12 | 0.05 | 0.47 | 0.09 |
| **G20** | $D_h$ (nm)[b] | 27 | 39 | 67 | 137 | 108 | 202 |
| | PDI[c] | 0.35 | 0.21 | 0.22 | 0.26 | 0.22 | 0.25 |

[a] Apparent Z-average hydrodynamic diameter of the nanoparticles.

[b] Apparent polydispersity index of the nanoparticles.

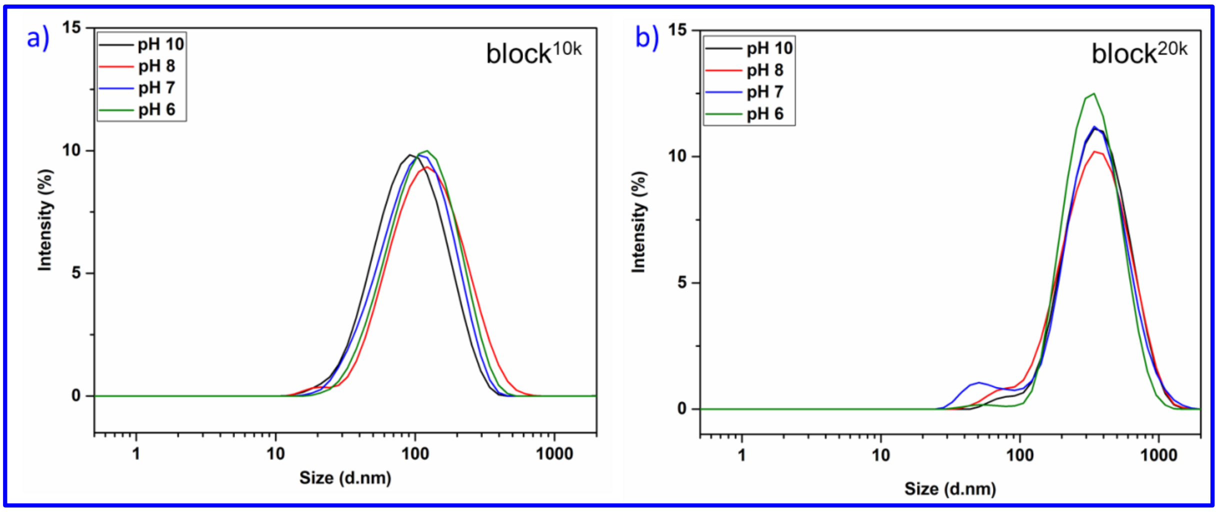

**Figure S20.** Size distributions obtained by DLS for block copolymers poly($BA_{50\%}$-*block*-$AA_{50\%}$) directly dispersed in different pH buffers: a) **B10** (10 kg $mol^{-1}$); b) **B20** (20 kg $mol^{-1}$)

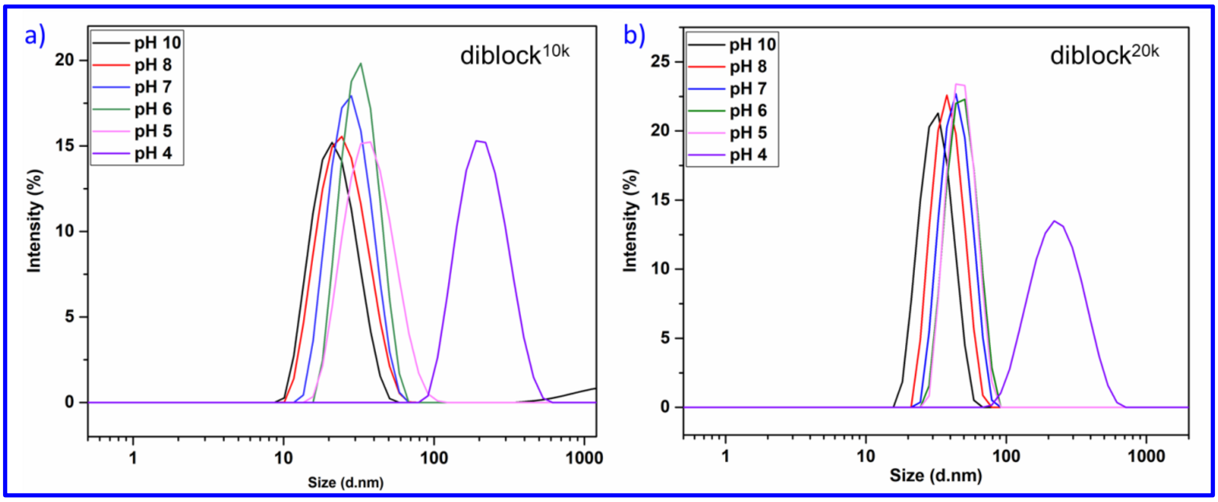

**Figure S21.** Size distributions obtained by DLS for the asymmetric diblock copolymers a) **D10** (10 kg $mol^{-1}$); b) **D20** (20 kg $mol^{-1}$). The low intensity, large diameter (≥400 nm) population observed at pH value 10 (**D10**) is most probably either due to contamination by dust particles or to a negligible weight fraction of spurious aggregates[S8,S9] as no corresponding structures were observed in cryoTEM.

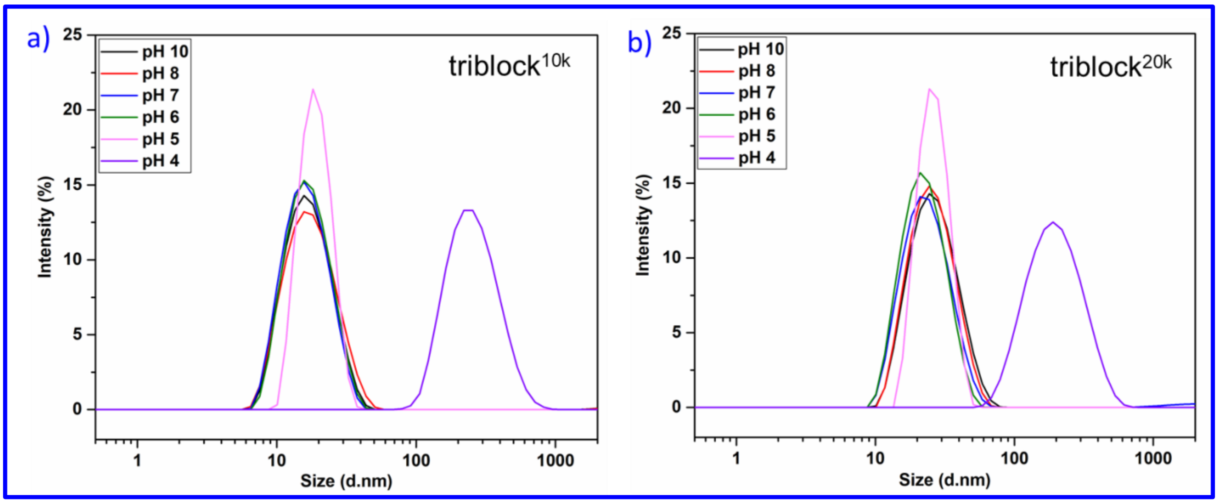

**Figure S22.** Apparent size distributions obtained by DLS for the asymmetric triblock copolymers a) **T10** (10 kg mol$^{-1}$); b) **T20** (20 kg mol$^{-1}$). The very low intensity, large diameter (≥1000 nm) population observed at pH value 7 (**T20**) are most probably either due to contamination by dust particles or to a negligible weight fraction of spurious aggregates[S8,S9] as no corresponding structures were observed in cryoTEM or at slightly higher or lower pH value.

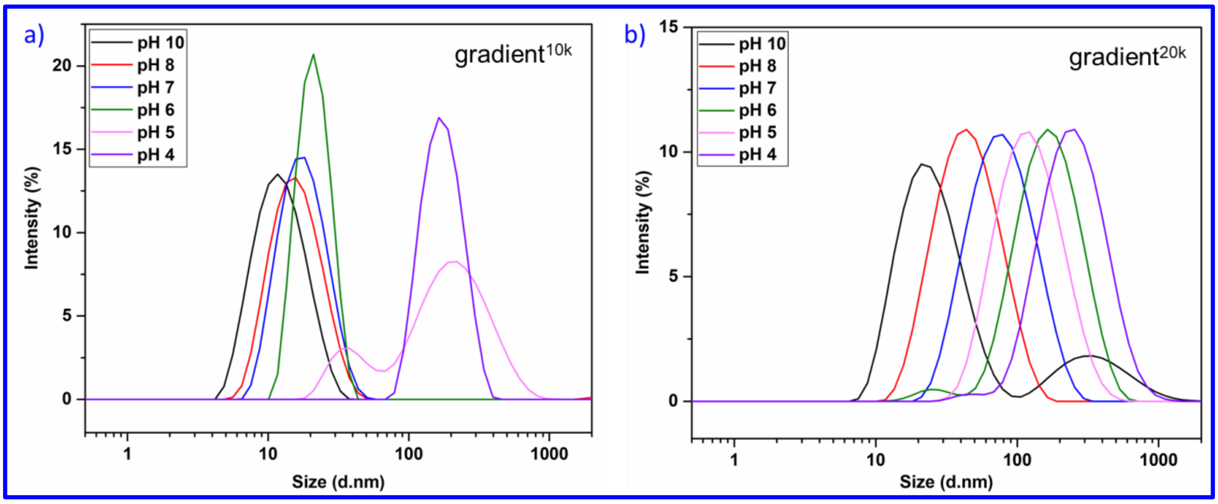

**Figure S23.** Apparent size distributions obtained by DLS for the gradient copolymers poly($BA_{50\%}$-*grad*-$AA_{50\%}$) directly dispersed in different pH buffers: a) **G10** (10 kg mol$^{-1}$); b) **G20** (20 kg mol$^{-1}$). The low intensity, large diameter (≥100 nm) population observed at pH value 10 (**G20**) is most probably either due to contamination by dust particles or to a negligible weight fraction of spurious aggregates[S8,S9] as no corresponding structures were observed in cryoTEM. The bimodal population observed at pH value 5 (**G10**) suggests the presence of a mixture of small and large aggregates. Due to the limitations of the fitting algorithm when applied to bimodal distributions, the distribution shown may not be an accurate representation of the true size distribution.

## 7. CRYOGENIC TRANSMISSION ELECTRON MICROSCOPY

### Additional CryoTEM Images for block copolymer B20

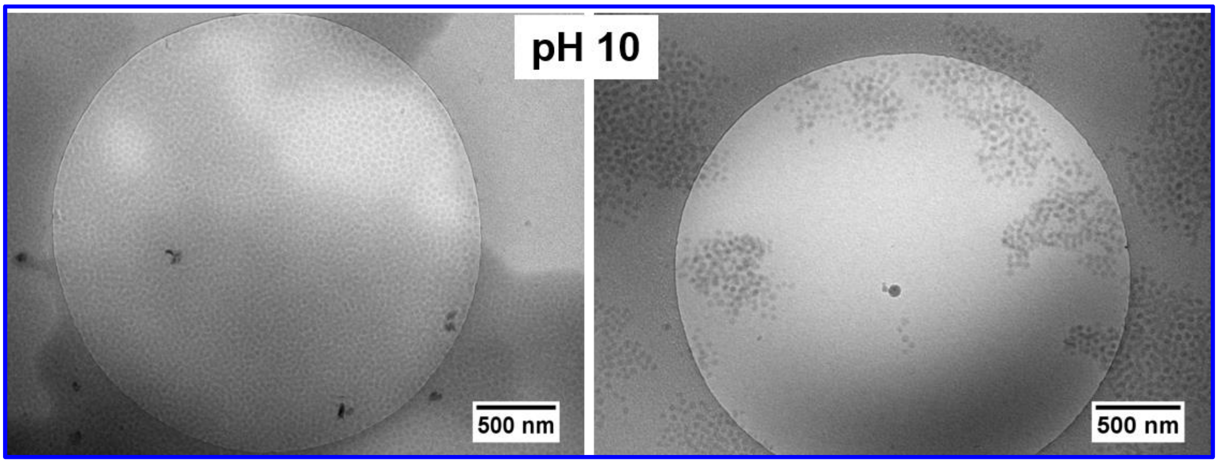

**Figure S24.** Cryo-TEM images of block copolymer **B20** (20 kg mol$^{-1}$) directly dispersed in the pH 10 buffer.

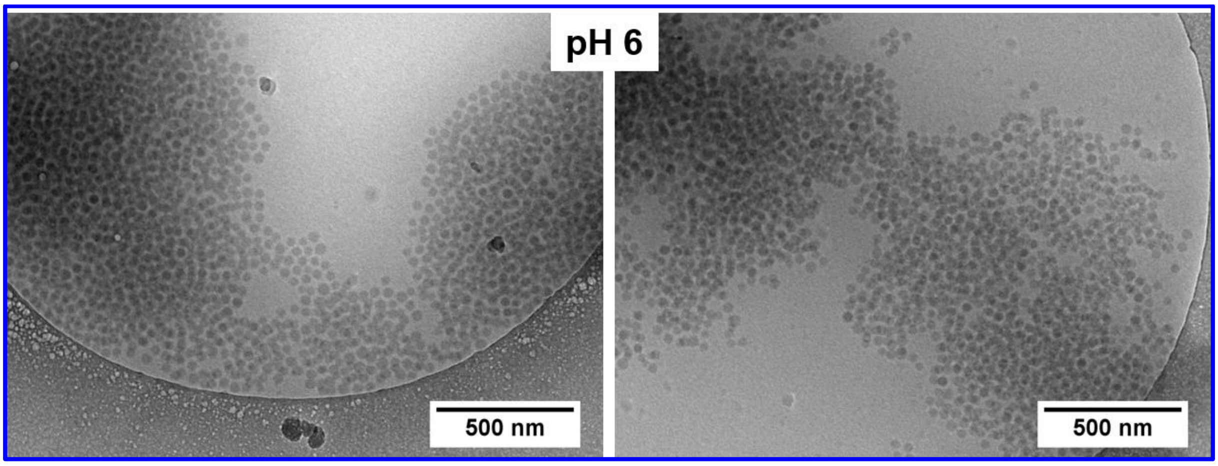

**Figure S25.** Cryo-TEM images of block copolymer **B20** (20 kg mol$^{-1}$) directly dispersed in the pH 6 buffer.

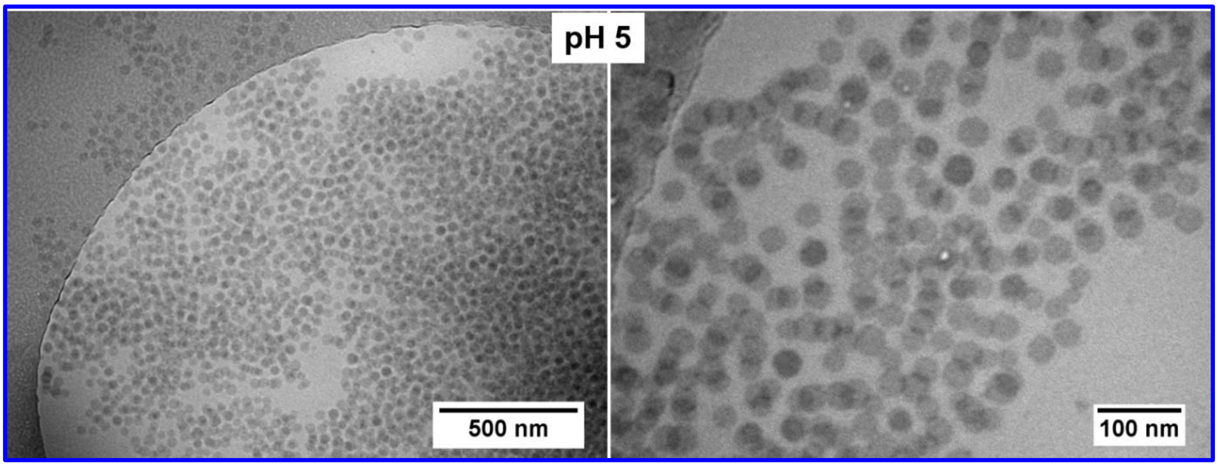

**Figure S26.** Cryo-TEM images of block copolymer **B20** (20 kg mol$^{-1}$) directly dispersed in the pH 5 buffer.

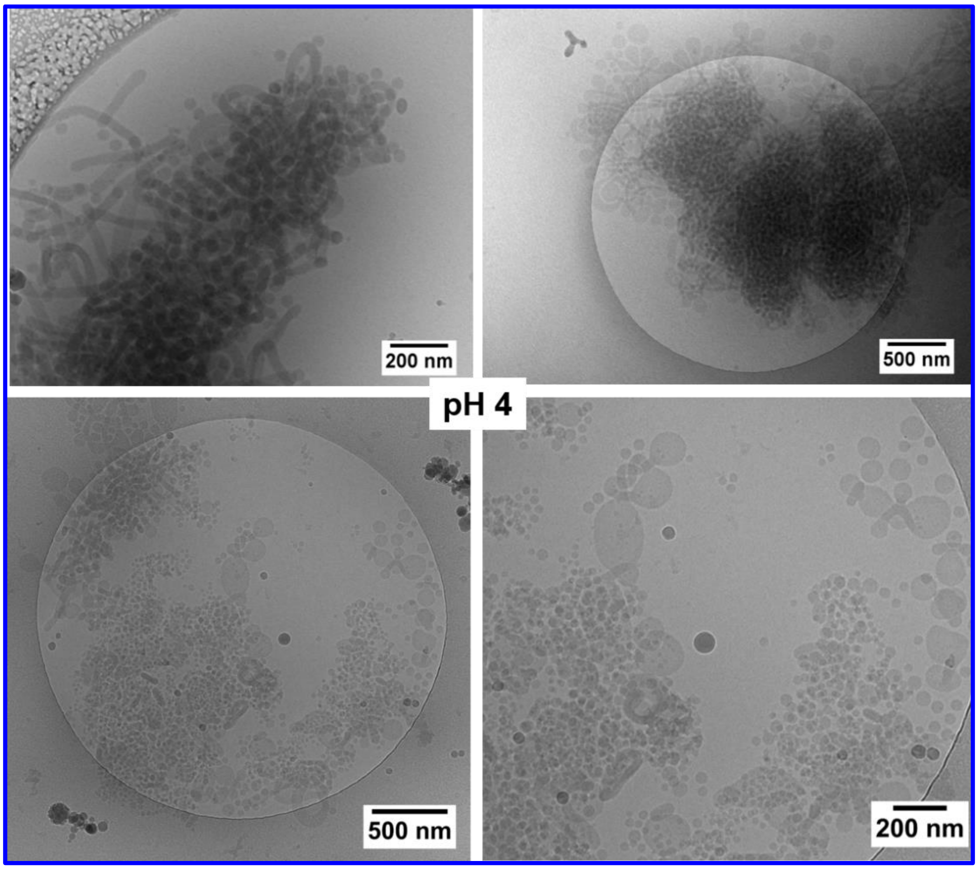

**Figure S27.** Cryo-TEM images of block copolymer **B20** (20 kg mol$^{-1}$) directly dispersed in the pH 4 buffer.

## Additional CryoTEM images: asymmetric diblock D10

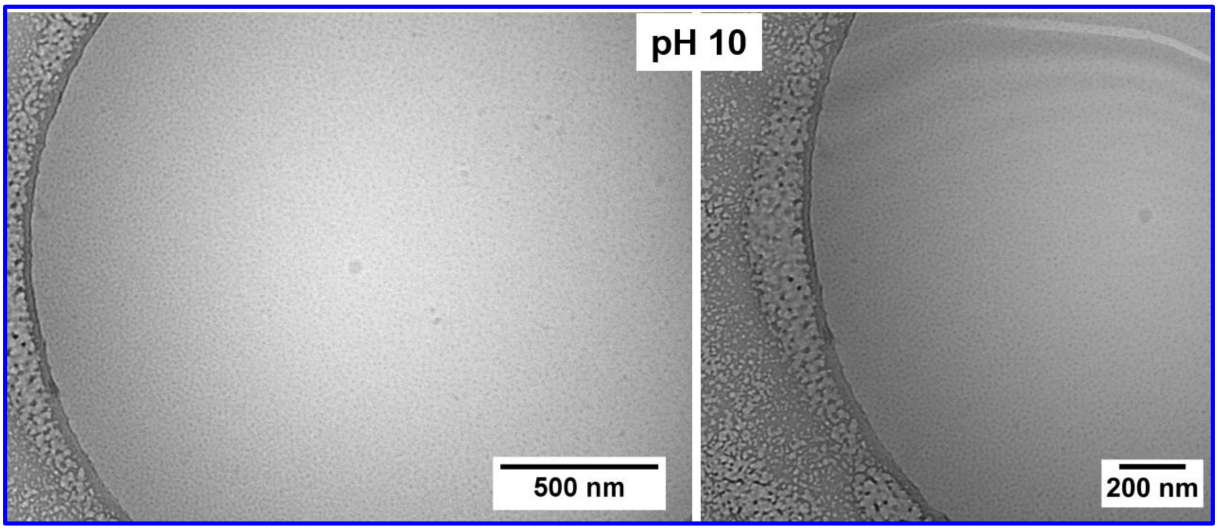

**Figure S28.** Cryo-TEM images of the asymmetric diblock copolymer **D10** (10 kg mol$^{-1}$) directly dispersed in the pH 10 buffer.

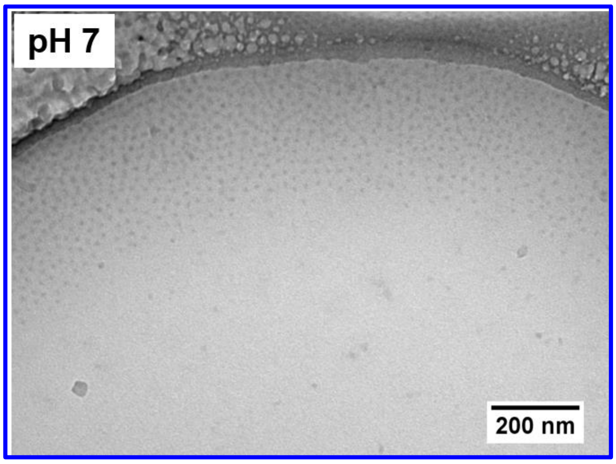

**Figure S29.** Cryo-TEM image of the asymmetric diblock copolymer **D10** (10 kg mol$^{-1}$) directly dispersed in the pH 7 buffer.

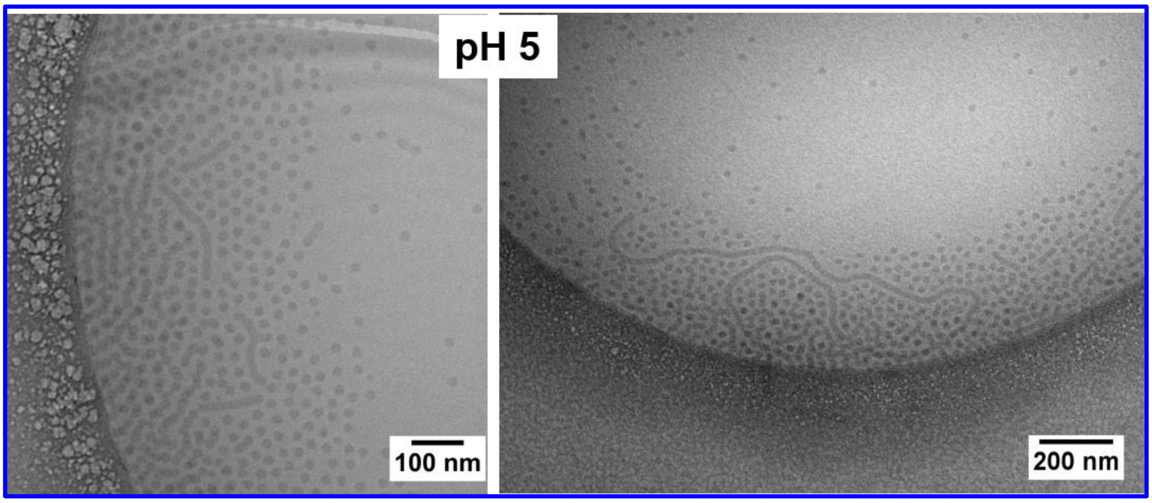

**Figure S30.** Cryo-TEM image of the asymmetric diblock copolymer **D10** (10 kg mol$^{-1}$) directly dispersed in the pH 5 buffer.

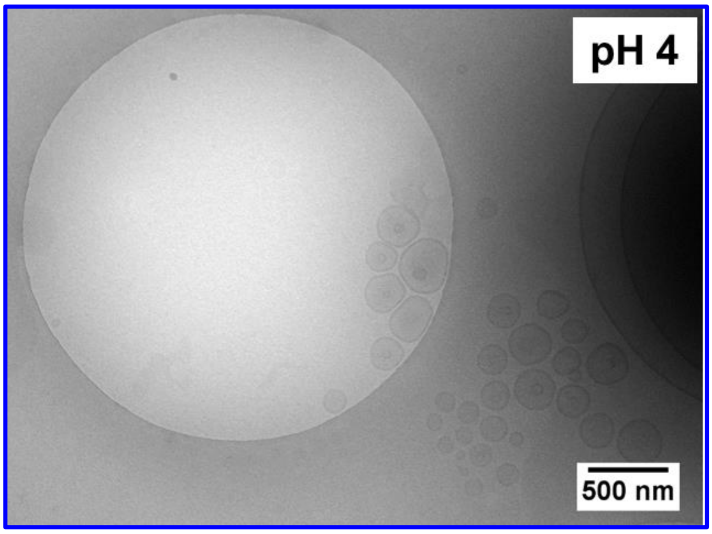

**Figure S31.** Cryo-TEM image of the asymmetric diblock copolymer **D10** (10 kg mol$^{-1}$) directly dispersed in the pH 4 buffer.

**Additional CryoTEM images: asymmetric triblock copolymer T10**

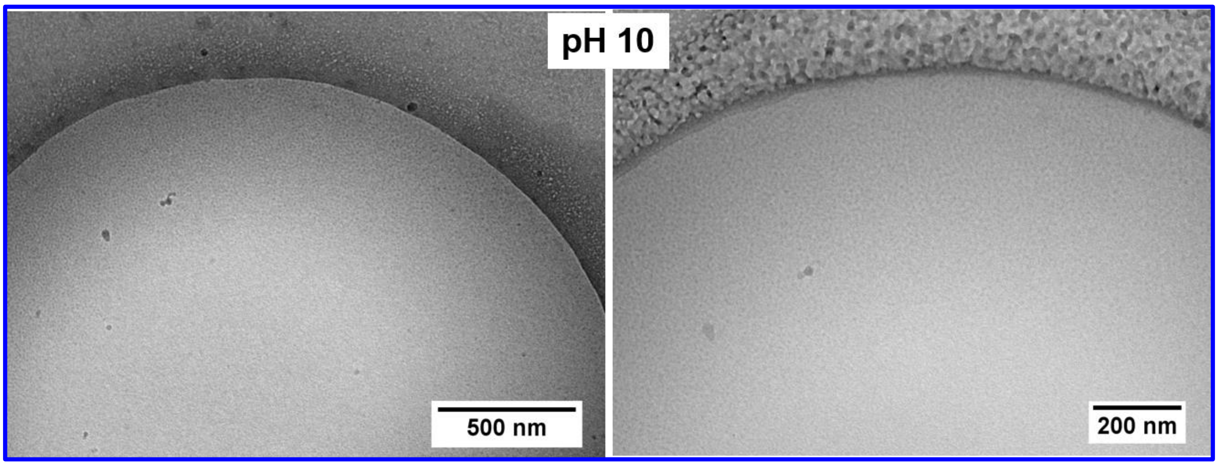

**Figure S32.** Cryo-TEM image of the asymmetric triblock copolymer T10 (10 kg mol$^{-1}$) directly dispersed in the pH 10 buffer.

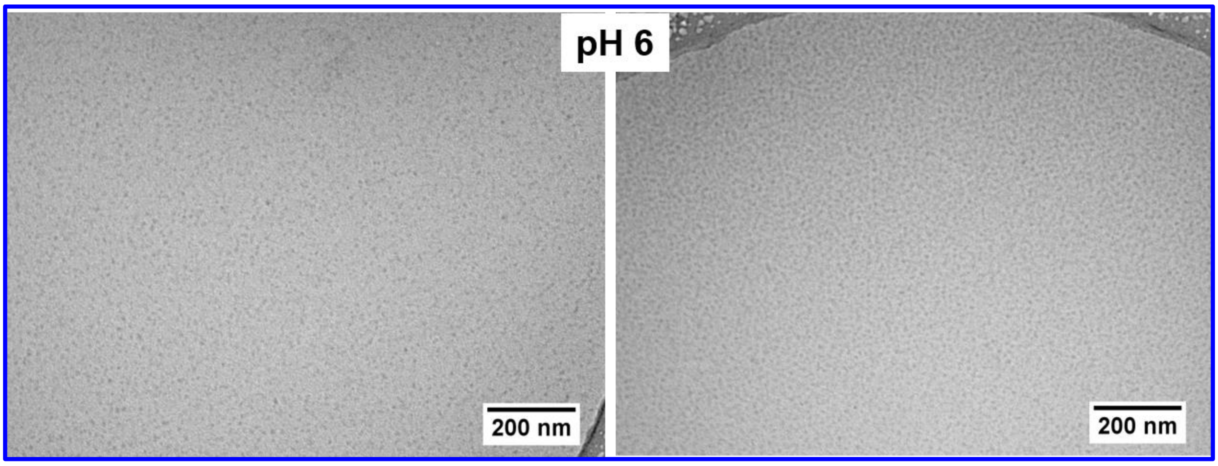

**Figure S33.** Cryo-TEM images of asymmetric triblock copolymer T10 (10 kg mol$^{-1}$) directly dispersed in the pH 6 buffer.

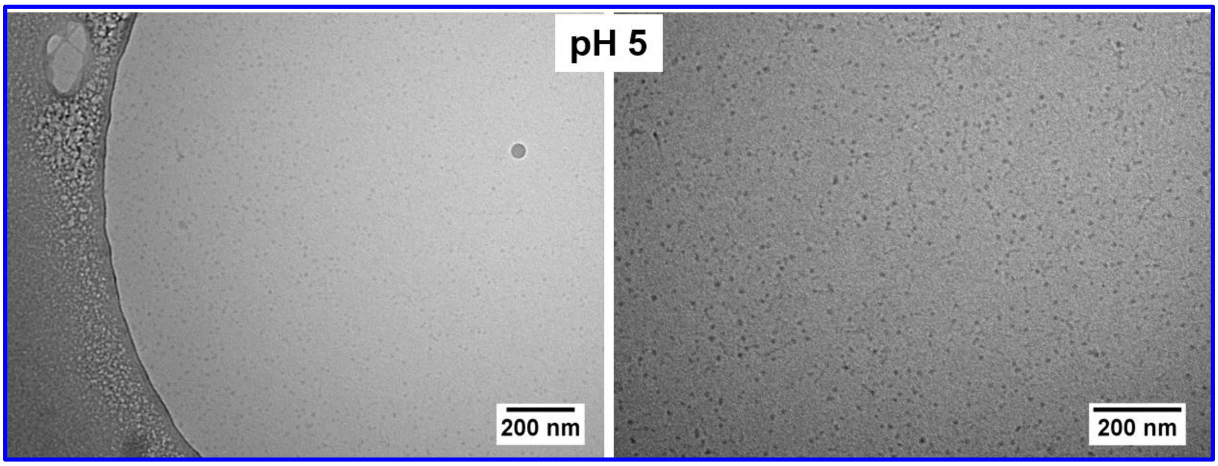

**Figure S34.** Cryo-TEM images of asymmetric triblock copolymer T10 (10 kg mol$^{-1}$) directly dispersed in the pH 5 buffer.

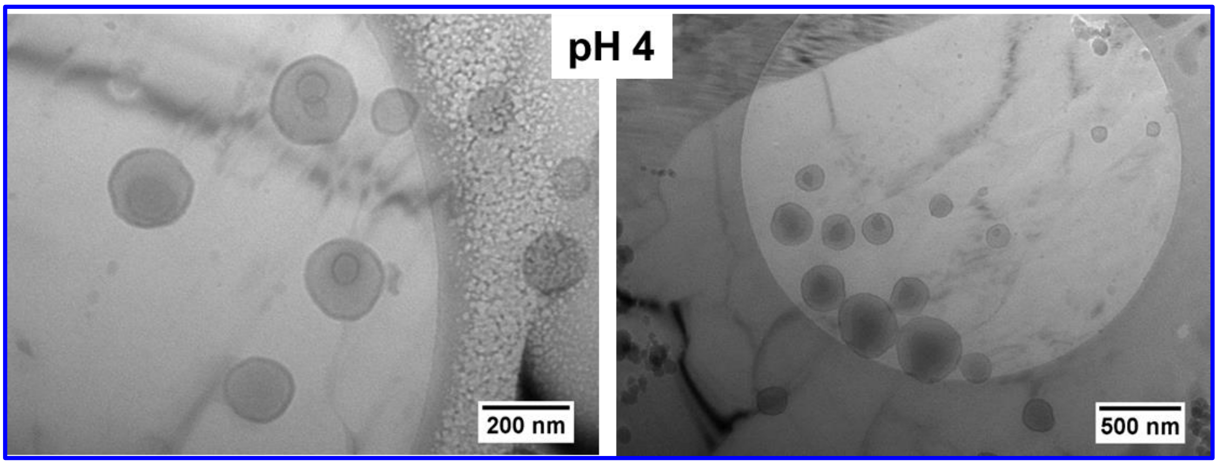

**Figure S35.** Cryo-TEM images of the asymmetric triblock copolymer T10 (10 kg mol$^{-1}$) directly dispersed in the pH 4 buffer.

## Additional CryoTEM images: gradient copolymer G20

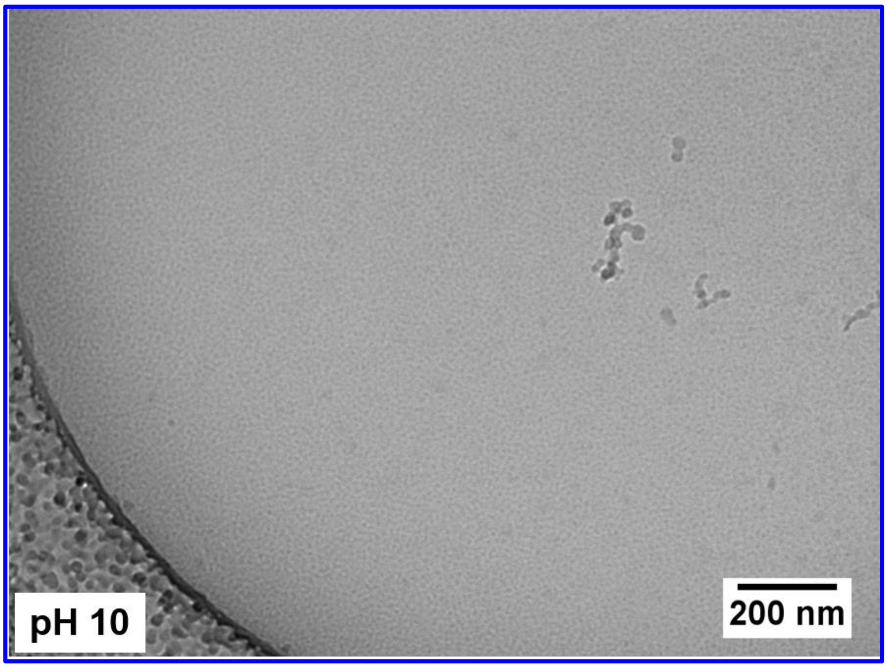

**Figure S36.** Cryo-TEM image of gradient copolymer **G20** (20 kg mol$^{-1}$) directly dispersed in the pH 10 buffer.

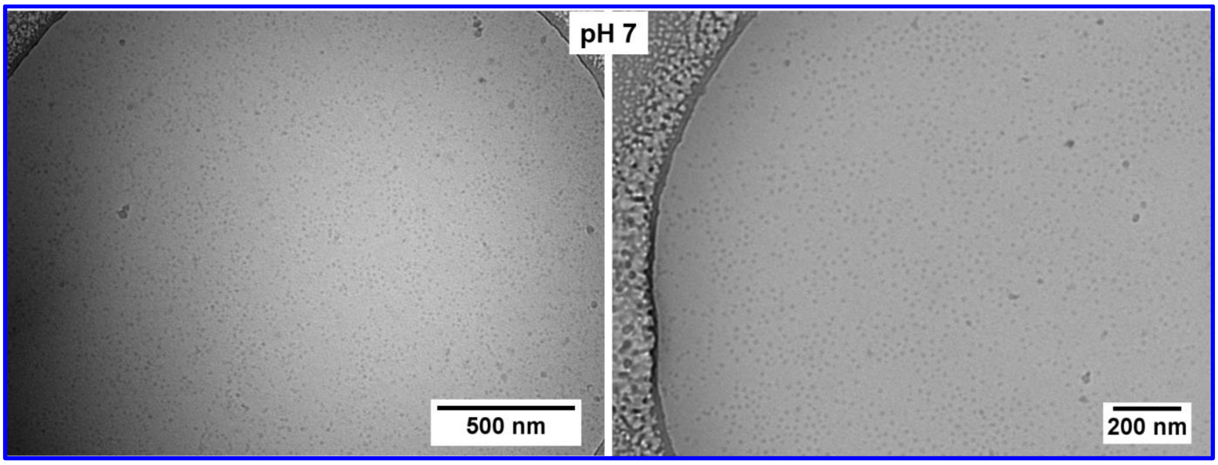

**Figure S37.** Cryo-TEM images of the gradient copolymer **G20** (20 kg mol$^{-1}$) directly dispersed in the pH 7 buffer.

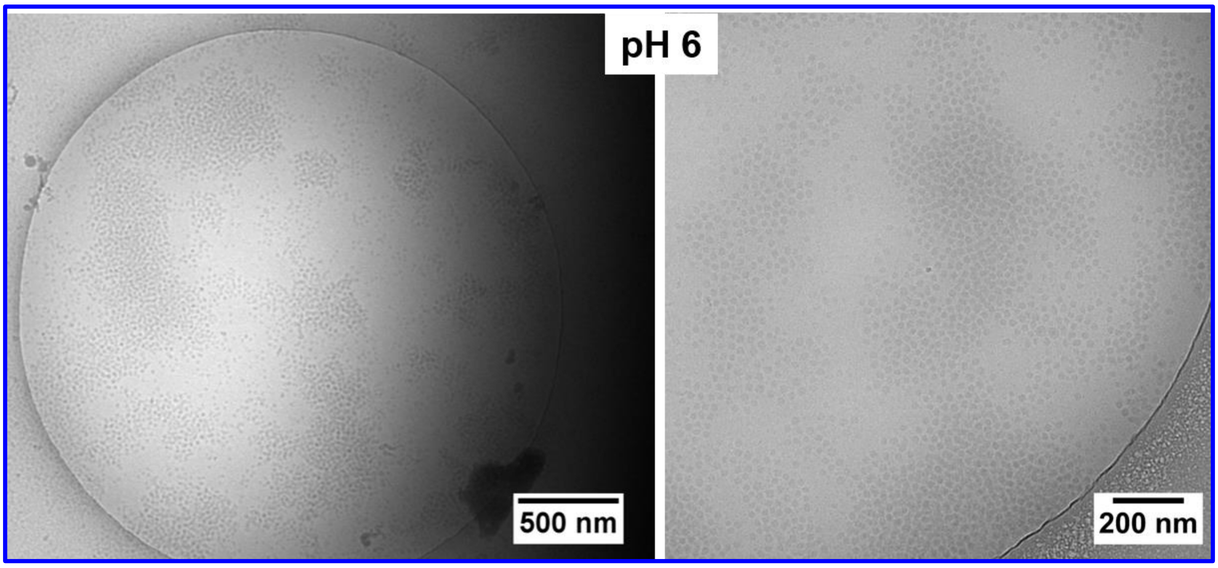

**Figure S38.** Cryo-TEM images of the gradient copolymer **G20** (20 kg mol$^{-1}$) directly dispersed in the pH 6 buffer.

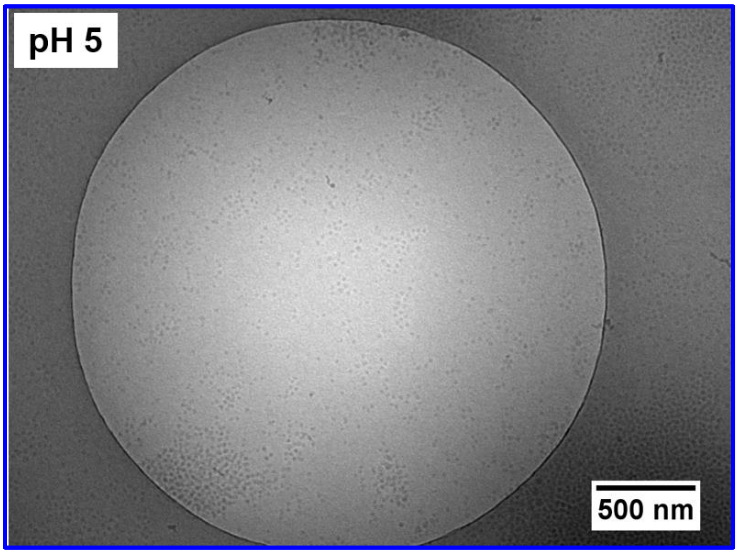

**Figure S39.** Cryo-TEM image of the gradient copolymer **G20** (20 kg mol$^{-1}$) directly dispersed in the pH 5 buffer.

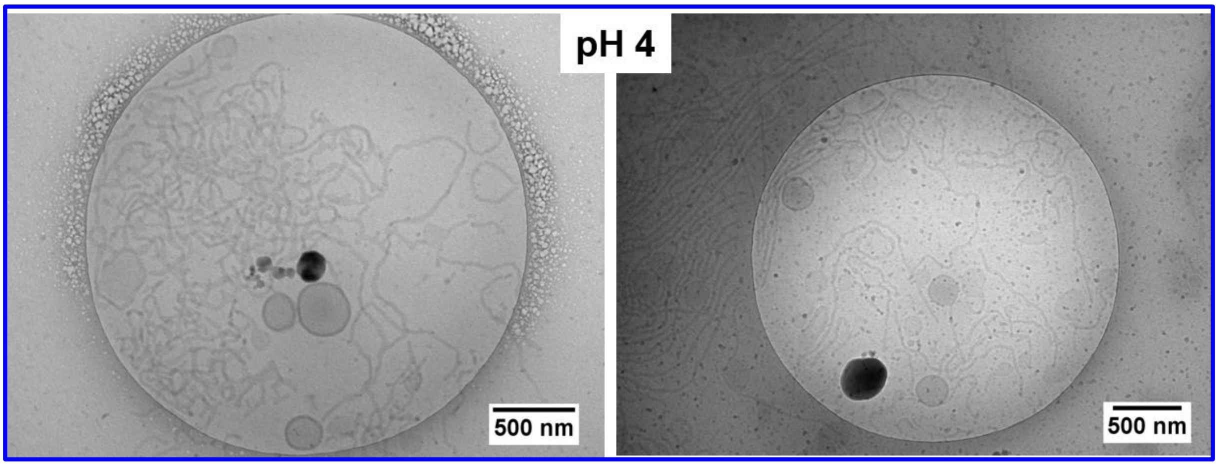

**Figure S40.** Cryo-TEM images of the gradient copolymer **G20** (20 kg mol$^{-1}$) directly dispersed in the pH 4 buffer.

## 8. SMALL ANGLE NEUTRON SCATTERING

From the scattering data of Figure 4, it is possible to evaluate the molar mass of the self-assemblies from the value of the forward scattering using the following formula obtained from the Guinier approximation:

$$I(q=0)=\frac{C\Delta\rho^2 M_W}{N_A\,d^2}$$

Where $C$ is the copolymer concentration, $\Delta\rho=\rho_{polymer}-\rho_{solvent}$ with $\rho_{polymer}$ and $\rho_{solvent}$ the scattering length density of the copolymer and the solvent, respectively, d the copolymer density, $N_A$ the Avogadro number and $M_w$ the molar mass of the nano-objects in solution.

The scattering data of **Figure 4** at pH values 5, 7 and 10 (asymmetric diblock copolymer **D10**) were fitted using a cylindrical model according to the following relationship for the particle form factor, *P(q)*, of randomly oriented particles:

$$P(q)=\int_0^{\pi/2}F^2(q,\alpha)\,sin\alpha\,d\alpha=\int_0^1 F^2(q,u)\,du \qquad \text{(S8)}$$

with

$$F(q)=\frac{2J_1(qR_c\sin\alpha)}{qR_c\sin\alpha}\frac{\sin(\frac{qL}{2}\cos\alpha)}{(\frac{qL}{2}\cos\alpha)} \qquad \text{(S9)}$$

*$J_1(x)$* represent the first order Bessel function, $R_c$ et $L$ are the radius and the length of the cylinder, respectively. The polydispersity of the radius and the length of the anisotropic assemblies was described with a Gaussian function.[S10]

At pH 5, the fit could be slightly improved by incorporating a contribution from spherical particles of radius 12 ± 2 nm, accounting for 6% of the total scattering intensity. A comparison of the two curves (cylinders + spheres *versus* cylinders only) is shown in Figure S41. While this indicates that the observed scattering is consistent with a mixture of cylindrical and spherical particles, the total scattering is dominated by the larger cylinders, and the parameters associated with contribution of the spherical particles should be interpreted with caution.

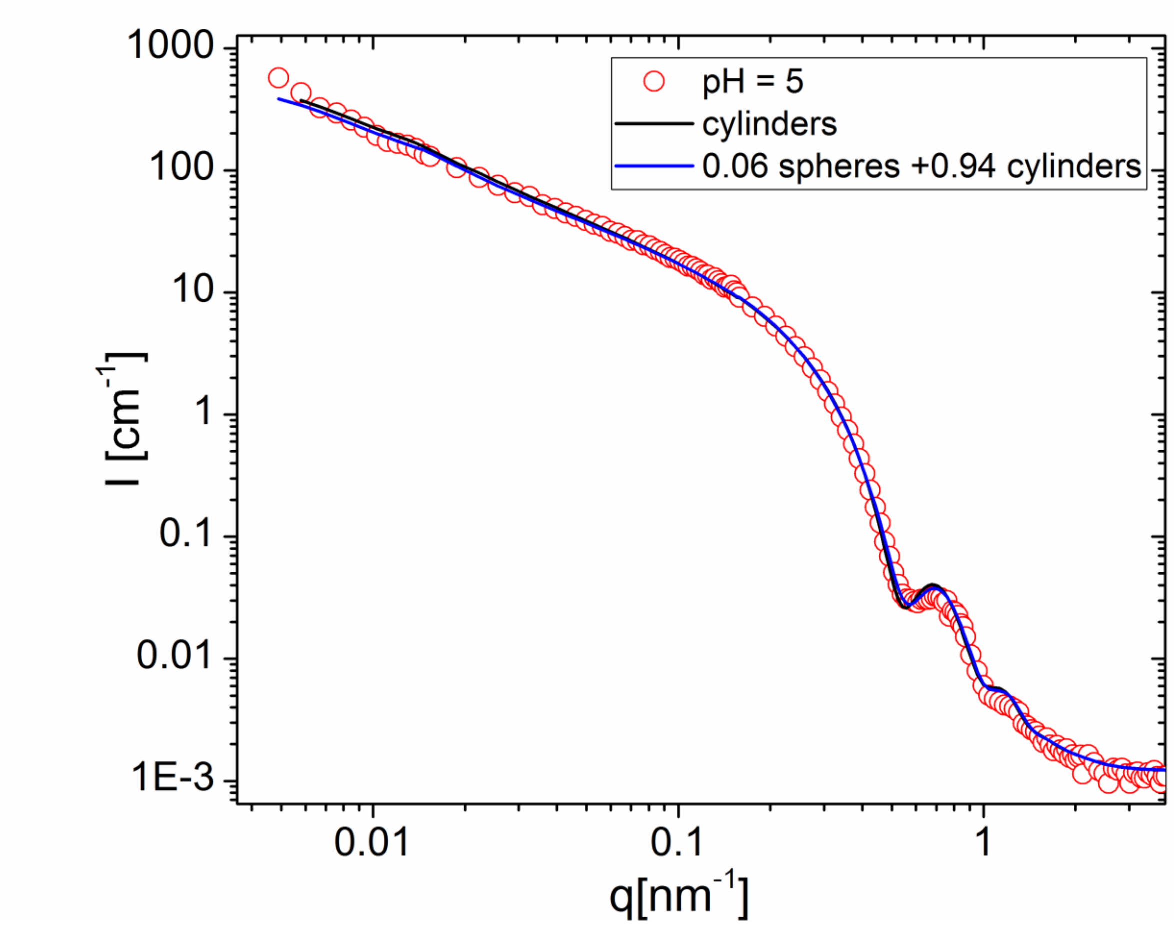

**Figure S41.** Comparison of cylinder only (black line) and cylinder + sphere (blue line) models applied to experimental neutron scattering data (open circles) from **D10** at pH 5.

At pH value 10 a contribution for free polymer chains had also to be added to the cylinder model in order to account for the scattering intensity at high q. A model for polymer chains undergoing excluded volume interactions was used. The analytical form developed by Hammouda[S11] is:

$$P(q) = \frac{1}{\nu U^{1/2\nu}}\,\gamma\left(\frac{1}{2\nu}, U\right) - \frac{1}{\nu U^{1/\nu}}\gamma\left(\frac{1}{\nu}, U\right) \tag{S10}$$

with $\gamma(x, U) = \int_0^U dt\; e^{-t} t^{x-1}$

and $U = \frac{q^2 R_g^2 (2\nu+1)(2\nu+2)}{6}$

$R_g$ is the polymer gyration radius and ν the excluded volume parameter (equal to 3 in our case).

At pH value 4, the vesicles were described as hollow spheres. A core-shell spherical model was used where the core was replaced by the solvent to account for the presence of the internal aqueous pool and the shell was the polymer bilayer:

$$F(q) = \frac{3}{V_{TOT}}\left[\frac{V_c(\rho_s-\rho_{sh})j_1(qR_c)}{qR_c} + \frac{V_{TOT}(\rho_{sh}-\rho_s)j_1(qR_{TOT})}{qR_{TOT}}\right] \qquad \text{(S11)}$$

$V_{TOT}$ is the volume of the whole nano-object, $V_c$ is the volume of the core (aqueous pool), $R_C$ is the radius of the core (aqueous pool) and $R_{TOT} = R_c + d$ (d is the shell thickness), $\rho_s$ and $\rho_{sh}$ are the scattering length density of the solvent and the shell respectively. $j_1$ is the first order spherical Bessel function. The polydispersity of the radius and the length of the anisotropic assemblies was described with a Gaussian function.

The presence of other morphologies (worm-like micelles for example) as shown by cryo-TEM images is the reason that the model does not exactly reproduce the data. However, the main features (the bilayer size at q ~ 0.6 $nm^{-1}$ and the overall size at q ~ 0.25 $nm^{-1}$) of the vesicles could be described.

**Table S12.** Values of the characteristic sizes (in nm) of the nano-objects according to fit results. $R_v$ and $d$ are the radius and the bilayer thickness of the vesicles (written as mean values ± standard deviation). $L$ and $R_c$ are the length and radius of the elongated micelles, long or flexible cylinders. $K_L$ is the Kuhn length of the flexible cylinders. $R_g$ is the gyration radius of the single polymer chains.

| **pH value** | | | |
|---|---|---|---|
| **4** | Vesicles | $R_v$ | 89±20 |
| | | $d$ | 11±2 |
| **5** | Long cylinders[a] | $L$ | > 600 |
| | | $R_c$ | 7.1±0.5 |
| **7** | Elongated micelles | $L$ | 17±2 |
| | | $R_c$ | 5.1±0.5 |
| **10** | Elongated micelles | $L$ | 14.0±0.5 |
| | | $R_c$ | 3.50±0.2 |
| | Polymer chains | $R_g$ | 2.5±0.2 |

[a] A slightly improved fit could be obtained by incorporating a contribution from spheres of radius 12±2 nm, accounting for 6% of the total scattering intensity.

Figure S42 shows the SANS curves relative to B20 at the two extreme pH values investigated (pH value 4 and 10).

At both pH values a power-law behavior, I(q) α q-x with x= 2.9 and 2.5 for pH value 10 and 4 respectively, is observed indicating the presence of fractal clusters whose size exceed the one accessible in our experiment (size bigger than 1 µm). The lower size measured through DLS experiments is due to the fact that they were conducted on filtered solution, so the obtained values are those of the bigger clusters which passed through filters (400 nm).

A peak is visible at intermediate q values, more pronounced in the case of pH value 10. This is expected as the correlation peak must be due to electrostatic interactions and the polymer is almost neutral at pH value 4.

Both curves could be described as polydisperse spheres densely packed in fractal aggregates.[S12] To emulate the effect of electrostatic interactions, we used a hard sphere model allowing the excluded radius to be larger than the particle radius, adding a transparent shell of constant thickness.[S13-S15]

$$I(q) = I_{pHS}(q) \cdot S_f(q) \tag{S12}$$

A simple structure factor for fractals has been used

$$S_f(q) = 1 + aq^{-b} \tag{S13}$$

The exponent b is close to the fractal dimension $D_f$ of the aggregates.

The values for the fits are reported in Table S13 and are in good agreement with the cryo-TEM images (Figures 3, S24-40).

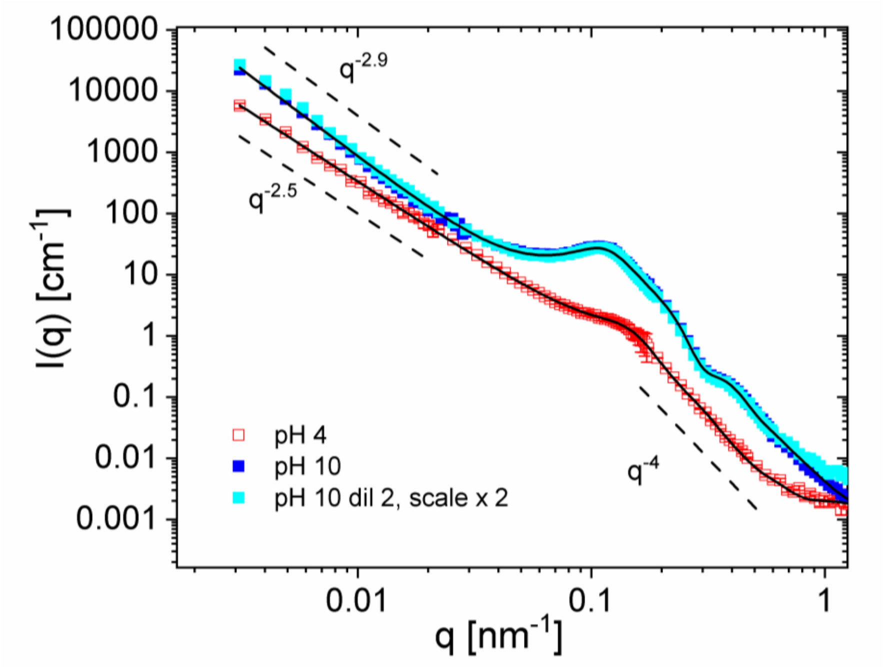

**Figure S42**. Small angle neutron scattering patterns for B20 at two different pH: 4 and 10. The black lines are the fitting curves using the models detailed in the text.

Interestingly, dilution at pH value 10 has no effect on the structure of the clusters, it just has the effect to dilute them (as the overall scattering intensity decreases proportionally to the concentration). Macroscopic phase separation occurs at pH value 4, meaning that the scattering spectra are representative of the polymer left in solution.

**Table S13.** Values of the fit parameters of the nano-objects formed. for **B20** at pH value 4 and 10. b is the power-law exponent; $R_c$ and ($R_c$ + $R_s$) are the spherical micelles radius and the center to center distance between adjacent micelles in the clusters; $\phi$ is the volume fraction inside the clusters

| | **pH value 10** | **pH value 4** |
|---|---|---|
| **b** | 2.87 | 2.47 |
| **$R_c$ (nm)** | 13.8±2.5 | 7.7±1.8 |
| **$R_s$ (nm)** | 10.9 | 11.2 |
| **$\phi$** | 0.04 | 0.016 |

## 9. REFERENCES:

S1 O. Colombani, E. Lejeune, C. Charbonneau, C. Chassenieux and T. Nicolai, *J. Phys. Chem. B*, **2012**, *116*, 7560–7565

S2 B. Lonetti, B. Farias-Mancilla, C. Guerrero Sanchez, S. Harrisson and S. Prévost, Asymmetric, gradient-like block-copolymers: solution behaviour as a function of pH. Institut Laue-Langevin (ILL), **2018**, doi:10.5291/ILL-DATA.9-11-1877

S3 U. Keiderling, The new 'BerSANS-PC' software for reduction and treatment of small angle neutron scattering data *Appl Phys A* **2002**, *74*, s1455–s1457

S4 C. Guerrero-Sanchez, S. Harrisson and D. J. Keddie, *Macromol. Symp.*, **2013**, *325–326*, 38–46.

S5 R. Yañez-Macias, I. Kulai, J. Ulbrich, T. Yildirim, P. Sungur, S. Hoeppener, R. Guerrero-Santos, U. S. Schubert, M. Destarac, C. Guerrero-Sanchez and S. Harrisson, *Polym. Chem.*, 2017, **8**, 5023–5032.

S6 J. J. Haven, C. Guerrero-Sanchez, D. J. Keddie and G. Moad, *Macromol. Rapid Commun.*, 2014, **35**, 492–497.

S7 J. J. Haven, C. Guerrero-Sanchez, D. J. Keddie, G. Moad, S. H. Thang and U. S. Schubert, *Polym. Chem.*, 2014, **5**, 5236–5246.

S8 J. P. Patterson, M. P. Robin, C. Chassenieux, O. Colombani and R. K. O'Reilly, *Chem. Soc. Rev.* **2014**, *43*, 2412-2425.

S9 a) S. Han, E. Nicol, F. Niepceron, O. Colombani, S. Pensec and L. Bouteiller, *Macromol. Rapid Commun.*, **2019**, *40*, 1800698 b) C. Charbonneau, M. M. D. S. Lima, C. Chassenieux, O. Colombani, T. Nicolai, *Phys. Chem. Chem. Phys.* **2013**, *15*, 3955; c) E. Lejeune, C. Chassenieux, O. Colombani, "pH induced desaggregation of highly hydrophilic amphiphilic diblock copolymers", in Trends in colloid and interface science XXIV, Springer, **2011**, p. 7.; d) C. Lefay, B. Charleux, M. Save, C. Chassenieux, O. Guerret, S. Magnet, *Polymer* **2006**, *47*, 1935

S10 J. Pedersen, *Adv. Colloid Interface Sci.* **1997**, *70*, 171-210

S11 B Hammouda & M-H Kim, *J. Molecular Liquids* **2017**, *247*, 434-440

S12 M. Muthig, S. Prévost, R. Orglmeister and M. Gradzielski, *J. Appl. Cryst.* **2013**, *46*, 1187-1195

S13 W.L. Griffith, R. Triolo, A.L. Compere, *Phys. Rev. A.* **1987**, *35*, 2200-2206

S14 L. Blum, G. Stell, *J. Chem. Phys.* **1979**, *71*. 42-46; L. Blum, G. Stell, *J. Chem. Phys.* **1980**, *72*, 2212 (erratum)

S15 W.L. Griffith, R. Triolo, A.L. Compere, *Physical Rev. A.*, **1986**, *33*, 2197-2000.